Reflection imaging for synthetic crosswell seismic data

Guoping Li and Robert R. Stewart

ABSTRACT

A complete processing procedure for crosswell reflection imaging is presented in this paper. The final result produced from this procedure is a depth stacked section. Before the stacked section can be generated, a number of intermediate steps need to be applied. After preprocessing, crosswell seismic data of multi-fold coverage are processed in common interval gathers to remove direct arrivals. In common interval gathers, reflected waves have sharp angles against the direct arrivals. This characteristic is useful when applying velocity filters to eliminate the direct arrivals. The data are then sorted into common source gathers, where upgoing and downgoing reflections have opposite dipping angles and therefore can be separated through f-k filtering. The crosswell reflection imaging is achieved by using the Common Reflection Point Stacking Method, whose theory is given in this paper. The common reflection point stacking method consists of sorting data into common reflection point gathers, applying horizontal and vertical moveout corrections, and stacking the CRP gathers. Velocity information is needed for these moveout corrections. To derive the velocity, a technique of velocity scanning is used in a zero interval gather. The CRP stacking method assumes a constant velocity medium and flat reflectors. The stacked wavefields for upgoing and downgoing reflections are combined, followed by a time-depth conversion. The processing procedure discussed in this paper is believed to provide an effective and simple way to handle a large crosswell seismic data set. To show this, synthetic crosswell reflection data consisting of 55 shots and 101 receivers were generated and processed following the procedure presented here. A study on real crosswell reflection seismic data imaging is given in a separate paper by Li and Stewart (1993).

INTRODUCTION

In the last decade, considerable interest has been shown in crosswell seismic data because of its potentially great resolution. Thus far, three basic methods of imaging with crosswell seismic data have been studied, including *tomographic inversions* (Peterson et al., 1985; Bregman et al., 1989; Lines and LaFehr, 1989; Lines and Tan, 1990; and Abdalla et al., 1990), *prestack migration* (Hu et al., 1988; Qin and Schuster, 1993; Zhou and Qin, 1993), and *stacking* (Stewart et al., 1991; Stewart and Marchisio, 1991; and Li and Stewart, 1992a, b). In addition, the well-known technique of crosswell-CDP mapping has been used in a number of crosswell reflection imaging studies (Abdalla et al., 1990; Lazaratos et al., 1991; Lazaratos et al., 1992; Khalil et al., 1993).

As in surface seismic CDP processing, a stacked section of crosswell seismic data of multi-fold coverage is desirable. But, few efforts were ever made in accomplishing such a stack section until recently (Stewart et al., 1991; Stewart and Marchisio, 1991). Some of the concepts that were used by Stewart et al. (1991) have been expanded by Li and Stewart (1992a, b). This new crosswell reflection imaging

method is composed of several major processing steps (Li and Stewart, 1992b), including: 1) removing direct arrivals in *common interval* (CI) gathers, 2) separating up- and down-going reflections in *common source* (CS) gathers, 3) deriving velocity information in a zero-interval CI gather, 4) applying vertical and horizontal moveout corrections in *common mid-depth* (CMD) gathers, and 5) stacking traces in *common reflection bin* (CRB) gathers to obtain the final stacked section. Since this method is, in many aspects, analogous to the surface seismic CDP processing techniques, its advantages in data processing are obvious.

However, a careful analysis reveals that if the seismic traces, with up- and down-going reflection wavefields already separated, are directly sorted into CRB gathers before VMO and HMO corrections are applied, use of the CMD gathers is found to be unnecessary. More importantly, this analysis leads to a new crosswell reflection imaging technique, which is referred to here as common reflection point (CRP) stacking method. As a result, the final stacked section resulting from the CRP stacking is equivalent to or even better than the stacked section obtained from the CMD-based processing procedure.

The CRP stacking method will be discussed in this paper. We will introduce some concepts used in the method. The important concepts will be demonstrated with synthetic crosswell data examples. A complete processing flow will be developed that may be used in processing real crosswell data. The application of this method to real crosswell seismic data acquired in Friendswood, Texas will be presented in a separate paper (Li and Stewart, 1993).

THEORY

The key to the CRP stacking method is to sort all seismic traces (after up- and down-going reflection separation) into a new data domain according to their common reflection point position, as shown in Figure 1(a). For a particular trace, the CRP position along a flat reflector is given by

$$L = \frac{X}{2}\left(1 + \frac{1}{2}\frac{g\text{-}s}{D\text{-}m}\right) , \qquad (1)$$

where L is the distance of the CRP measured from the source well, X is the borehole offset distance, g is the receiver depth, s is the source depth, D is the reflector depth, and m is the mid-depth of that trace (i.e., half of the sum of receiver and source depths). When the receiver and source depths are equal, the CRP is half way between the two boreholes.

In processing, a bin having a certain width is assigned to each CRP so that all traces falling into the same CRP bins are grouped into CRP gathers. Figure 1(a) illustrates the geometry of a CRP gather of N traces and Figure 1(b) shows its reflection time vs mid-depth curve. From the geometry shown, a relation between the time and depth can be derived:

$$t^2 = \left(t_0 - \frac{2m}{V}\right)^2 + \left(\frac{X}{V}\right)^2 , \qquad (2)$$

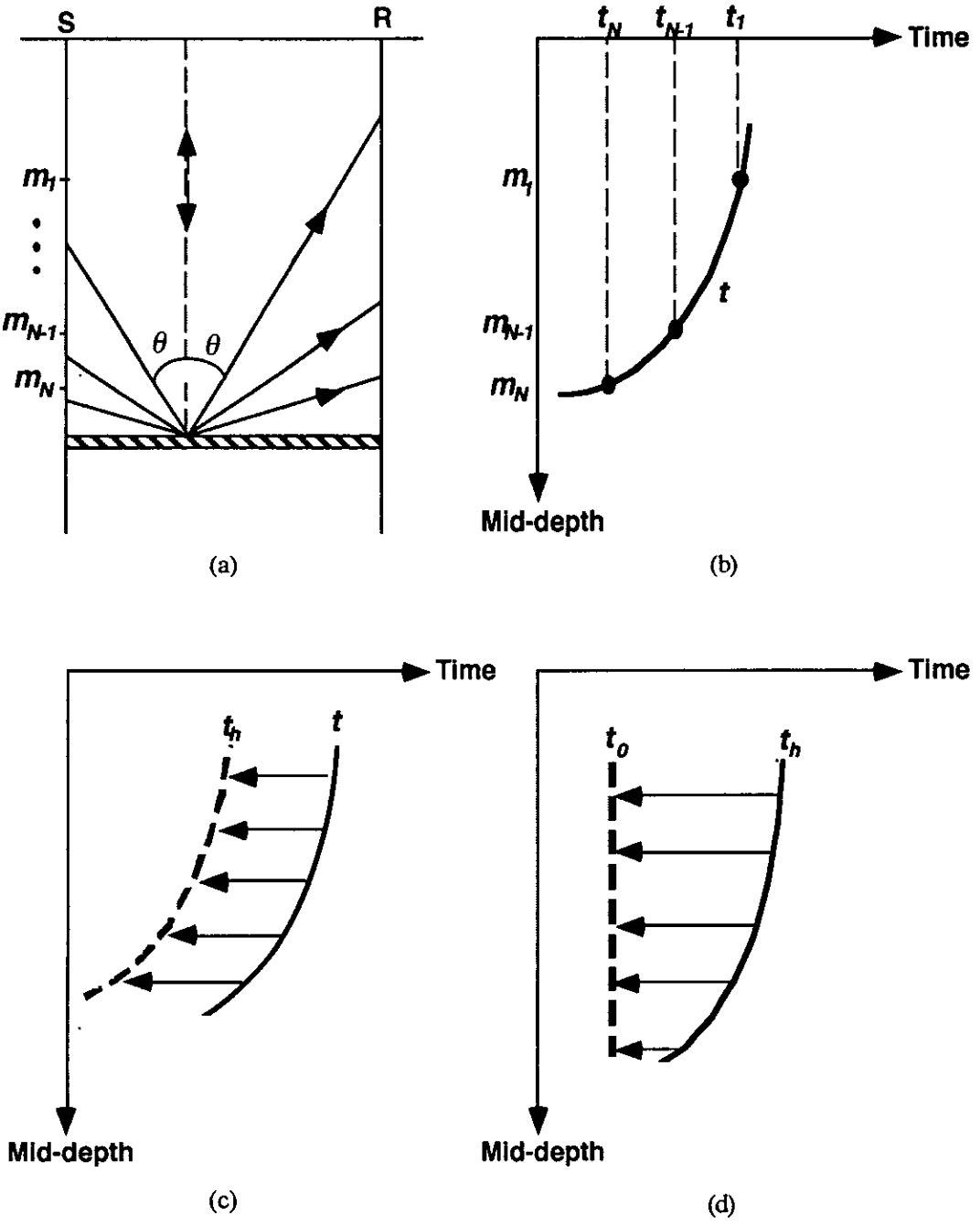

FIG. 1. Diagrams illustrating the geometry (a) and time-distance curve (b) of a common reflection point gather, the horizontal moveout correction (c) and the vertical moveout correction (d).

where t_0 is two-way vertical time from the reflector to the surface shown by the dashed line in Figure 1(a). Equation (2) implies a hyperbolic pattern of reflections in a CRP gather.

The second term on the right side of equation (2) is a constant since X is constant in the crosswell geometry and V is assumed a constant velocity. This term constitutes a time shift which corrects for horizontal moveout (HMO) due to the well-to-well distance X. If we make the following substitution in equation (2):

$$t_h = t_0 - \frac{2m}{V} , \tag{3}$$

then we have

$$t^2 = t_h^2 + \left(\frac{X}{V}\right)^2 . \tag{4}$$

So applying an HMO correction is equivalent to mapping the data from t to t_h, as shown in Figure 1(c).

After an HMO correction, we are left with a vertical moveout (VMO) determined by the term $2m/V$. Therefore the next necessary step obviously is a VMO correction. The VMO correction is calculated through the relation

$$t_0 = t_h + \frac{2m}{V} . \tag{5}$$

The process of VMO correction is shown in Figure 1(d). Applying both HMO and VMO corrections flattens the reflection event in a CRP gather. Then in a final processing step, we stack the traces over mid-depths to produce a stacked section.

Based on the above analysis, the CRP stacking method is composed of four steps: 1) Sorting separated reflection data into CRP gathers; 2) Correcting for horizontal moveout; 3) Correcting for vertical moveout; and 4) Stacking.

SYNTHETIC DATA GENERATION

To show these concepts, synthetic crosswell seismic data were generated from a simplified earth model shown in Figure 2. The geometry used here is similar to that of the Cold Lake crosswell seismic experiment shot by Imperial Oil Canada Ltd. However, a constant velocity medium was assumed. The model consists of five flat homogeneous layers, each having a different density and thickness. The constant velocity is 2250 m/s. The model is surrounded by a free surface and an infinitely large layer which has the same velocity but different density. So there are six horizons, numbered L1 to L6 from the top to the bottom, representing six reflectors. For example, the surface reflector is L1. The layer marked by a shadowed zone, which is bounded by reflectors L3 and L4, is the zone of interest. At the depth of 416.5 m is the top surface of this layer, which is to be imaged by crosswell reflections.

For the crosswell survey geometry, a well-to-well separation distance of 55 m was used. Fifty one sources were "shot" in the source well, ranging from 150 m to 450 m in depth, at intervals of 6 m. Signals were recorded at receiver position spanning

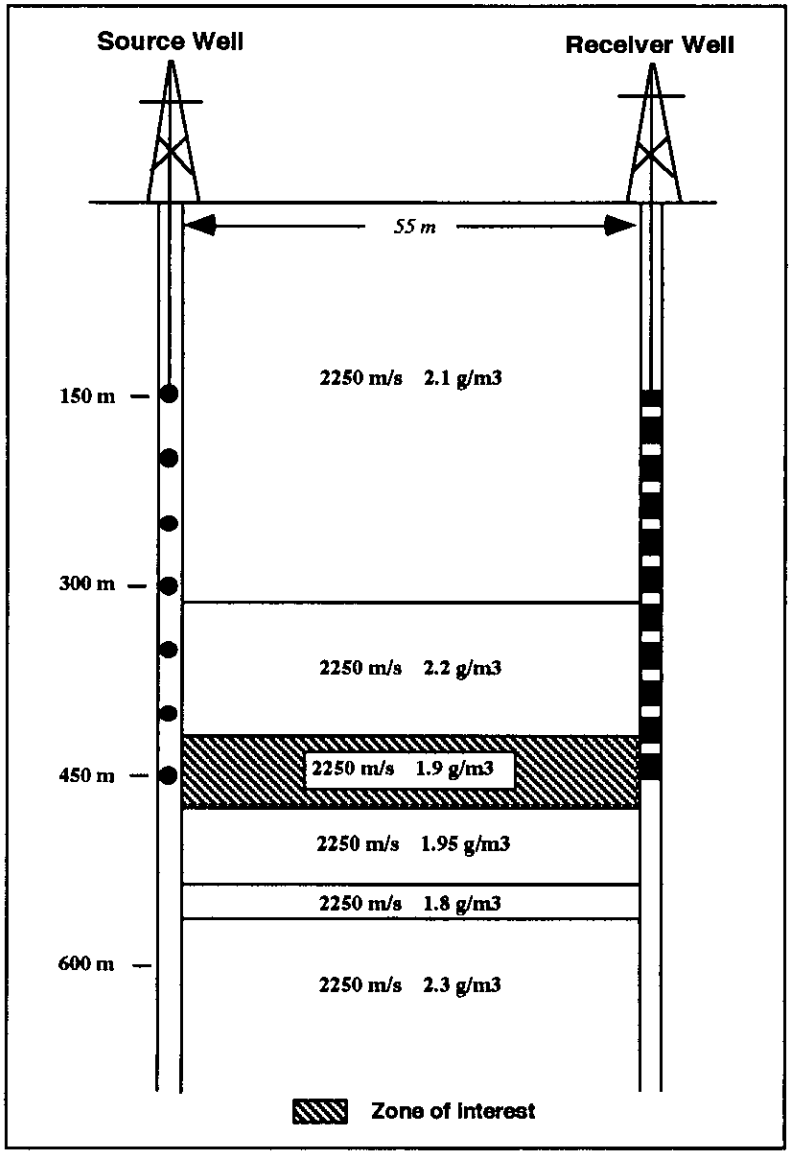

FIG. 2. Crosswell survey geometry and Earth model used to generate synthetic crosswell seismic data. Separation between boreholes is 55 m. The source was shot from 150 m to 450 m, at intervals of 6 m, while receiving geophones were deployed within a depth range of 150 m to 450 m, spaced at 3 m. The six reflectors, from the top to the bottom, are numbered L1 to L6, respectively. The target layer is the shadowed zone, bounded by horizons L3 and L4. Its top (L3), at depth of 416.5 m, will be imaged.

a depth range from 150 m to 450 m, spaced at 3 m. A 100 Hz zero-phase Ricker wavelet was used and only P-wave primary reflections and direct arrivals were simulated. The record length was 600 ms with a sampling interval of 1 ms.

A total of 51 shot records, each having 101 traces, were recorded. As examples, Figure 3 shows two typical common source gathers, corresponding to a source depth of 240 m and 360 m respectively. Only 0.4 seconds of data are displayed. In these gathers, a few features for direct arrivals and reflection events are observed. A hyperbolic direct arrival and a number of nearly linear reflections can be seen. The downgoing reflections have a down-to-left moveout whereas the upgoing reflections exhibit a down-to-right pattern. All of the 51 shot gathers were used in data processing and the results will be demonstrated in the following sections.

SYNTHETIC DATA PROCESSING AND IMAGING

Common source gather

Synthetic crosswell common source (CS) gathers have been shown in Figure 3. Although direct arrivals show an obvious hyperbolic pattern, the reflection events appear to be linear (see events L1, L3, and L4, for example). This is because we are looking at only a small portion of a large branch of the hyperbolic curve whose apex is far beyond the depth range shown here.

In common source gathers, reflected events often have larger moveouts than direct arrivals, a useful characteristic that makes separating direct waves from reflections by velocity filtering successful (Abdalla et al., 1990). However, sometimes applying a velocity filter to suppress direct arrivals in CS gathers may cause damages to reflections. Figure 4 shows such a case. There are two reflections below the hyperbolic direct arrival event: the downgoing reflection L2 and the upgoing reflection L3. Note that, above the depth of the source, reflection L3 has a moveout similar to that of the direct arrivals. It has been found (Iverson, 1988; and Pratt and Goulty, 1991) that this effect often occurs when both the source and the receiver are on the same side of the reflector and the receiver is farther away from the reflector than the source is, as indicated in Figure 4.

Applying a velocity filter to remove the direct arrivals from the CS gather in Figure 4 would affect not only the direct arrivals but also the reflections with similar moveouts, such as event L3. resulting in a greatly damaged reflection wavefield. A method to overcome this problem is to use common interval gathers, discussed next.

Common interval gather

A common interval (CI) gather collects those traces whose vertical depth interval between the source and the receiver is constant. In a constant velocity medium, direct arrivals in a CI gather are a flat event, while reflections are hyperbolic. This is confirmed in Figure 5, where three CI gathers are shown. Immediately above the upgoing and downgoing reflections, which have opposite dipping angles, are direct arrivals that are perfectly aligned. More importantly, notice the sharp termination of reflections against the direct arrivals, a useful characteristic possessed by CI gathers that can be employed in data processing. For example, we use CI gathers to remove direct arrivals from the total wavefield. Also, direct arrivals in CI gathers may be a useful indicator of velocity variation with depth for real crosswell seismic data, because

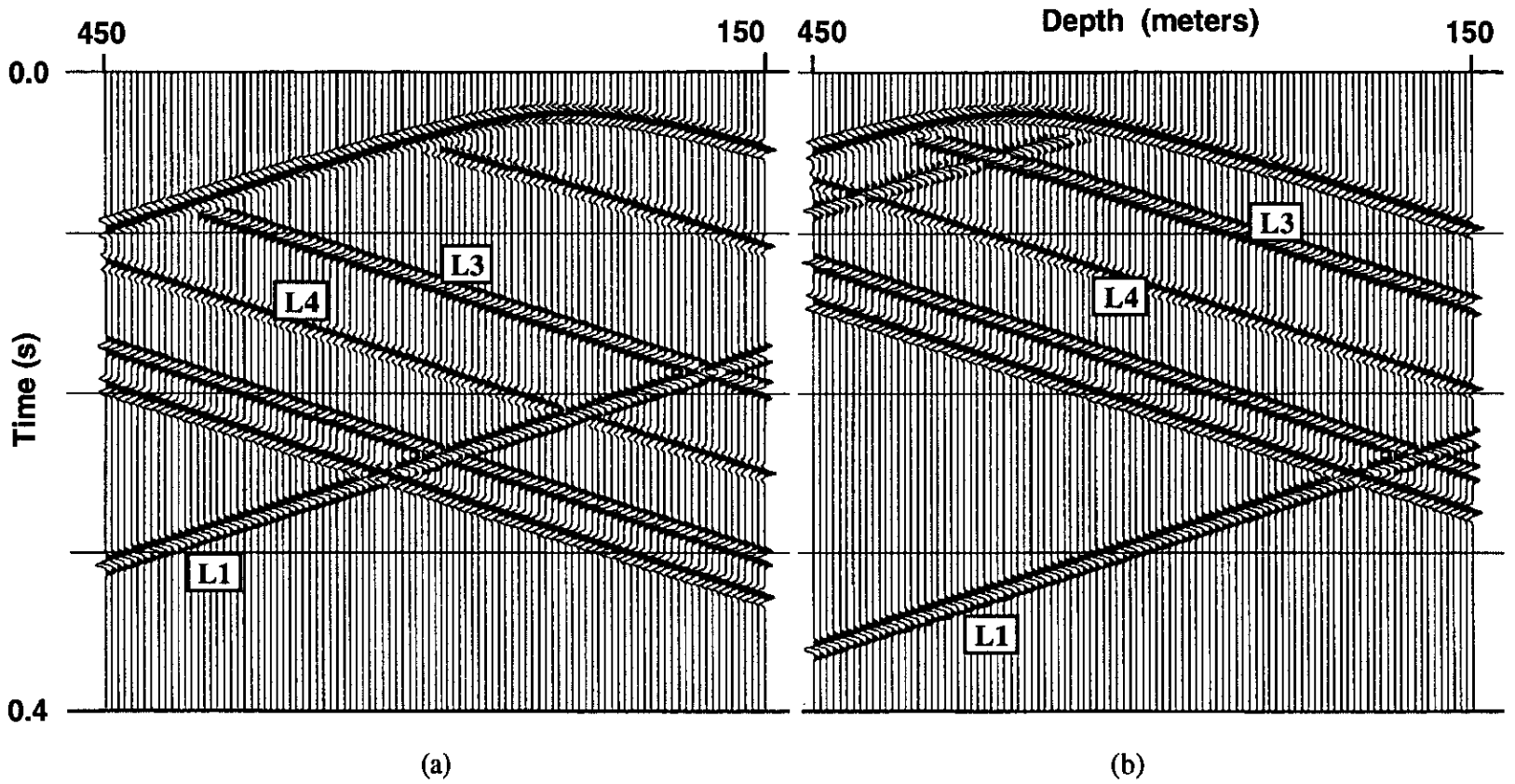

FIG. 3. Common source gathers generated from the crosswell geometry as in Figure 2. The source depths are 240 m (a) and 360 m (b), respectively. Each gather has 101 traces, representing recording depths from 150 m to 450 m, at intervals of 3 m. Events such as L3 and L4 are upgoing reflections, while events like L1 are downgoing reflections. The hyperbolic event is the direct arrival. L1 is a reflection from the top horizon, L3 and L4 are reflections from the top and bottom of the shadowed zone, in Figure 2.

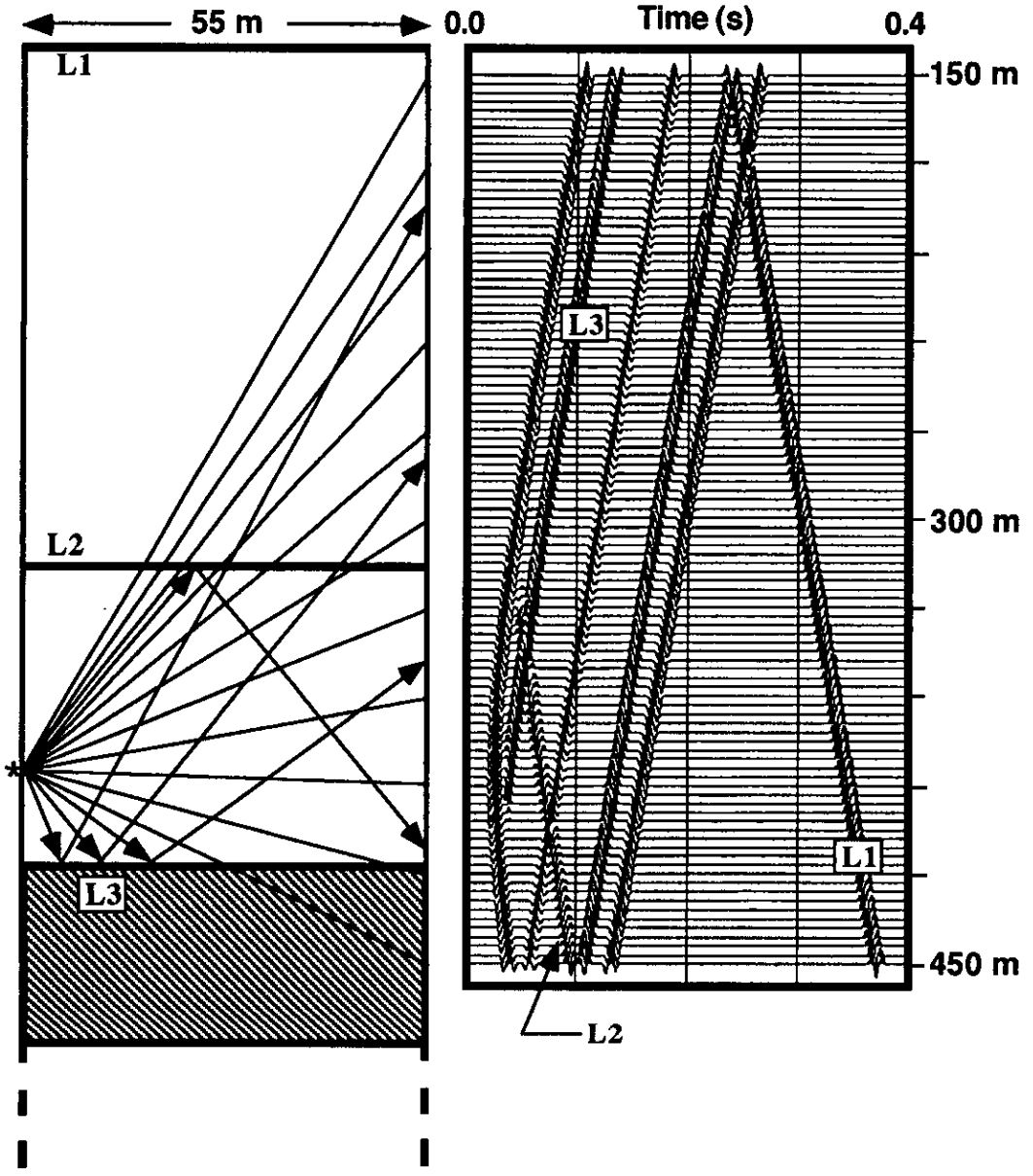

FIG. 4. When both the source and the receiver are on the same side of the reflector, and when the receiver is farther away from the reflector than the source, part of the hyperbolic direct wave will have a moveout that is very close to those of such reflection events as L3. In this case, applying velocity filters to remove the direct wave would damage the reflections.

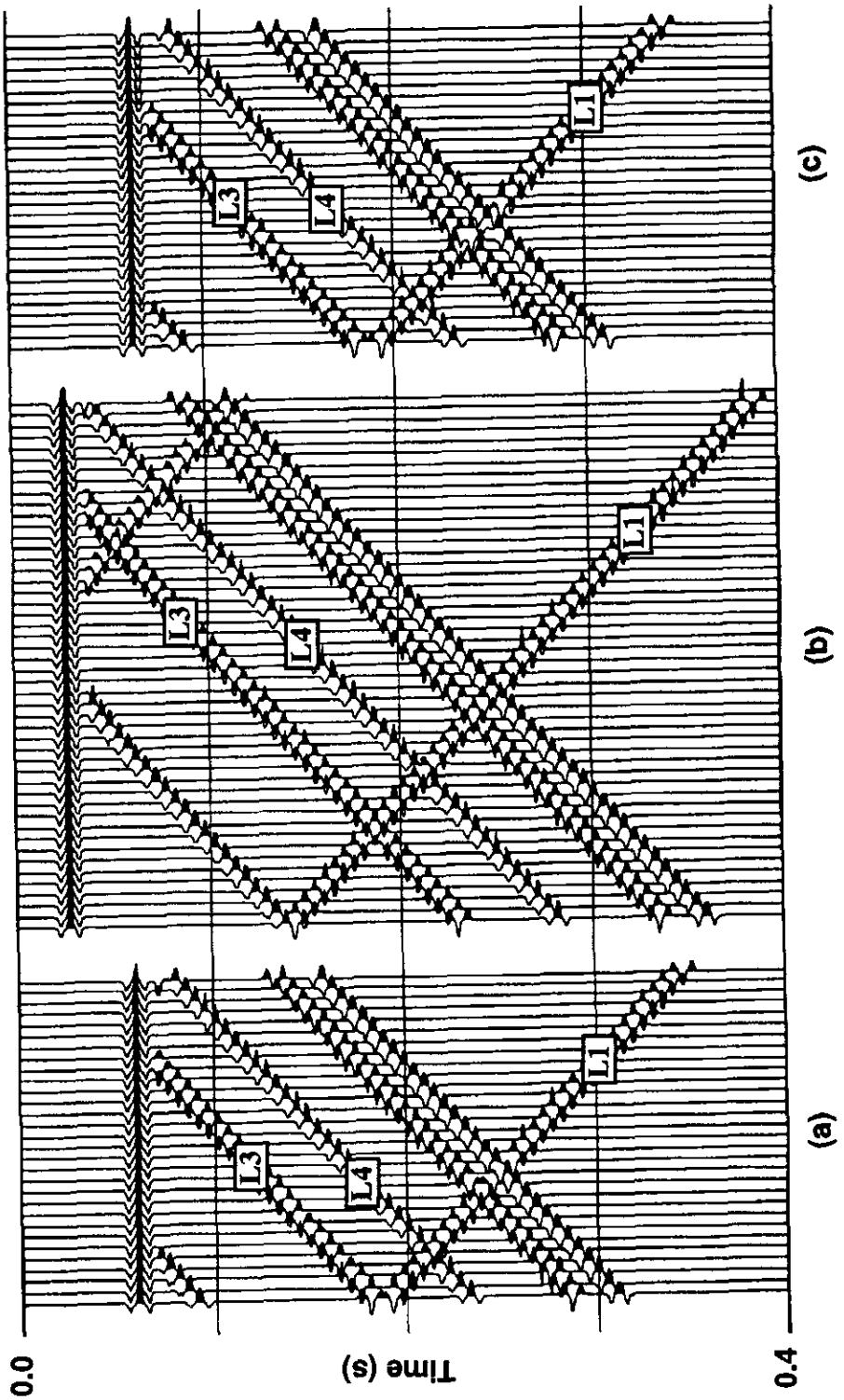

FIG. 5. Common interval gathers of synthetic crosswell seismic data. The vertical intervals between the source and the receiver for the gathers are 123 m (a), 18 m (b), and -132 m (c), respectively.

in real cases velocity changes with depth may affect the traveltimes of direct waves, thus affecting the flatness of these events in CI gathers.

Direct arrival removal

It is clear that, in the case of constant-velocity medium, crosswell direct arrivals are flat in CI gathers. These waves also have a sharp contact against the reflections. This characteristic enables us to apply a median filter to remove them from the total wavefield. Picking and time shifting the direct arrivals as done in the VSP data processing is unnecessary. The procedure is the following: the direct wave event in each CI gather is enhanced by median filtering with other waves removed, then the enhanced event is subtracted from the total wavefield. The result of doing this is the reflections that are retained. Figure 6 shows the reflection data after removing the direct waves (Figure 7) from the data in Figure 5. A median filter, whose operator is 11 traces long, was used. By comparing Figures 6 and 7 with Figure 5, it can be seen that the direct arrivals have been removed very nicely. Applying a median filter may cause some effect of high frequency glitch noise, which can be seen in the gathers in Figure 6. The problem of the glitches caused by median filtering can be overcome by running a high-cut filter after the median filtering (Stewart, 1985).

Figure 8 is the same CS gather as in Figure 4, but it has only reflections retained. The dash curve represents the position of the original direct arrival, which has been removed by median filtering in CI gathers. Note that no damage is made to the reflections through the filtering. It proves the advantage of separating the direct arrivals and reflections in the CI gathers.

Separation of up- and down-going reflections

After the direct arrivals have been removed, the filtered CI gathers are sorted back into CS gathers. An f-k filter could have been applied in the CI gathers to separate the upgoing and downgoing reflections. In these gathers, reflections have opposite apparent dips, which is an advantage to the f-k filter. However, as the vertical source-receiver interval becomes larger, there are fewer traces contained in a CI gather. As a result, the effect of f-k filtering would be less obvious in those gathers which do not have enough traces. Also the events might be aliased. Therefore, it is not recommended to separate upgoing and downgoing reflections in the CI gathers.

Wavefield separation can be done in CS gathers. Multichannel velocity filters such as an f-k filter can be used. Other filters like the median filter can also be applied but it involves time-consuming event picking. In this case, we chose to use the f-k filter. Figures 9 and 10 show, respectively, the upgoing reflections and downgoing reflections, separated from the same common source gather as in Figure 8. As can be seen, the f-k filter did a very good job. After the upgoing and downgoing reflections are separated, further processing leading to imaging can be performed on each mode of the reflection data.

Zero-interval velocity analysis

As discussed in a previous section, velocity information is needed when applying horizontal and vertical moveout corrections (equations (4) and (5)). Since we are assuming a constant velocity medium, the velocity used for HMO and VMO corrections should be identical. A crosswell velocity analysis method was presented by Li and Stewart (1992a, b). The concept of velocity scanning, which has been used in the surface seismic data processing to find the best NMO velocities in CDP gathers,was

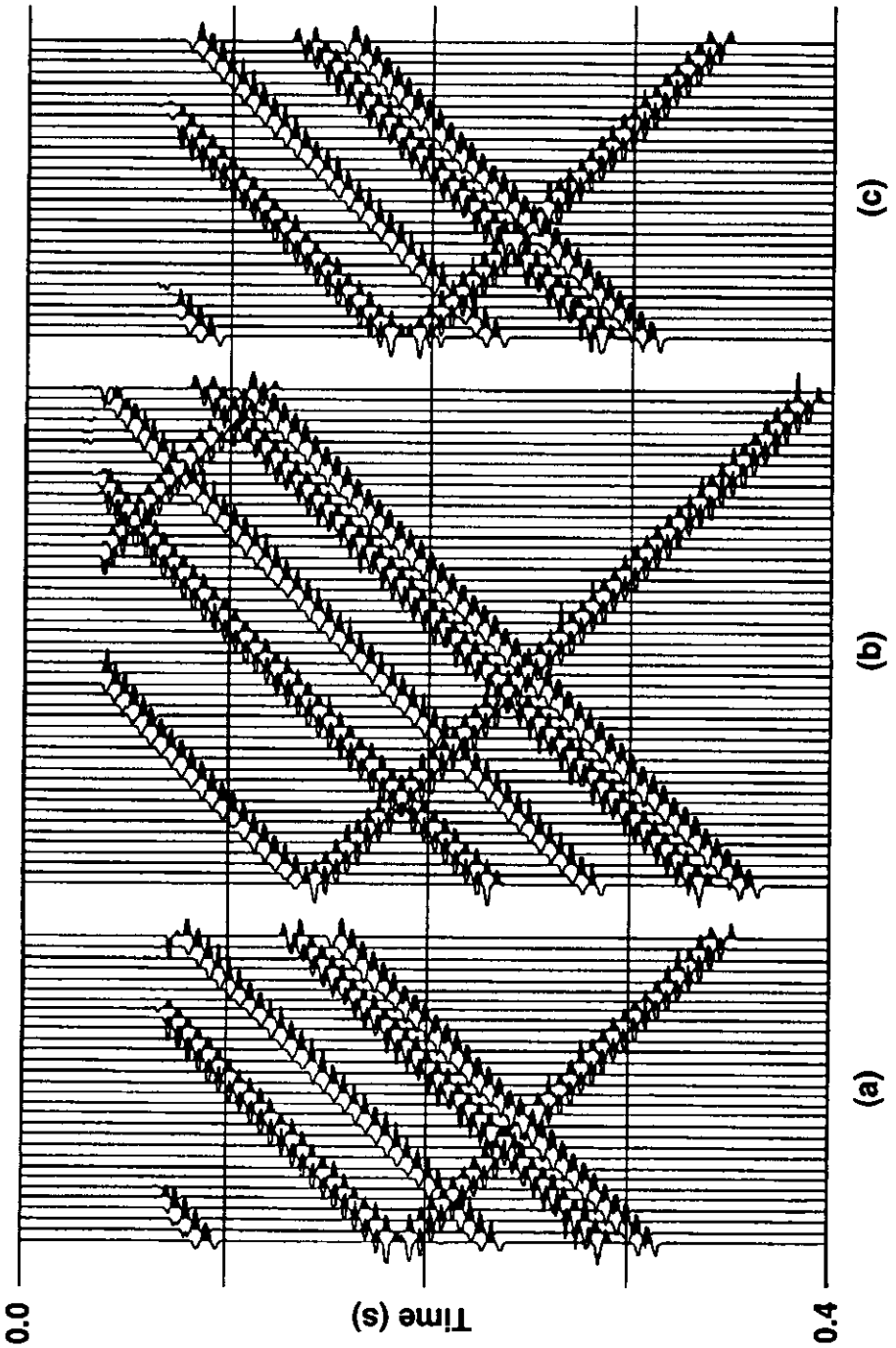

FIG. 6. Reflection data after removing direct arrivals by applying a median filter to the CI gathers of data in Figure 5. Gathers (a), (b), and (c) correspond to source-receiver intervals of 123 m, 18 m, and -132 m, respectively.

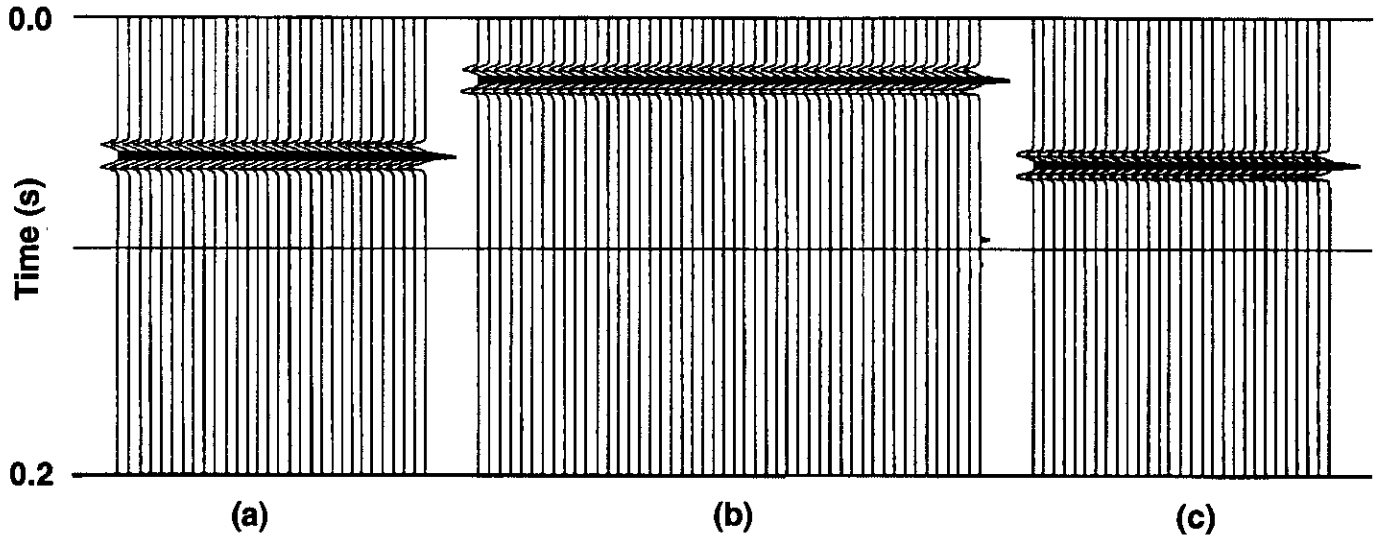

FIG. 7. Direct arrivals removed from the total wavefield in Figure 5, by running a median filter in the CI gathers. The filter operator length is 11 traces.

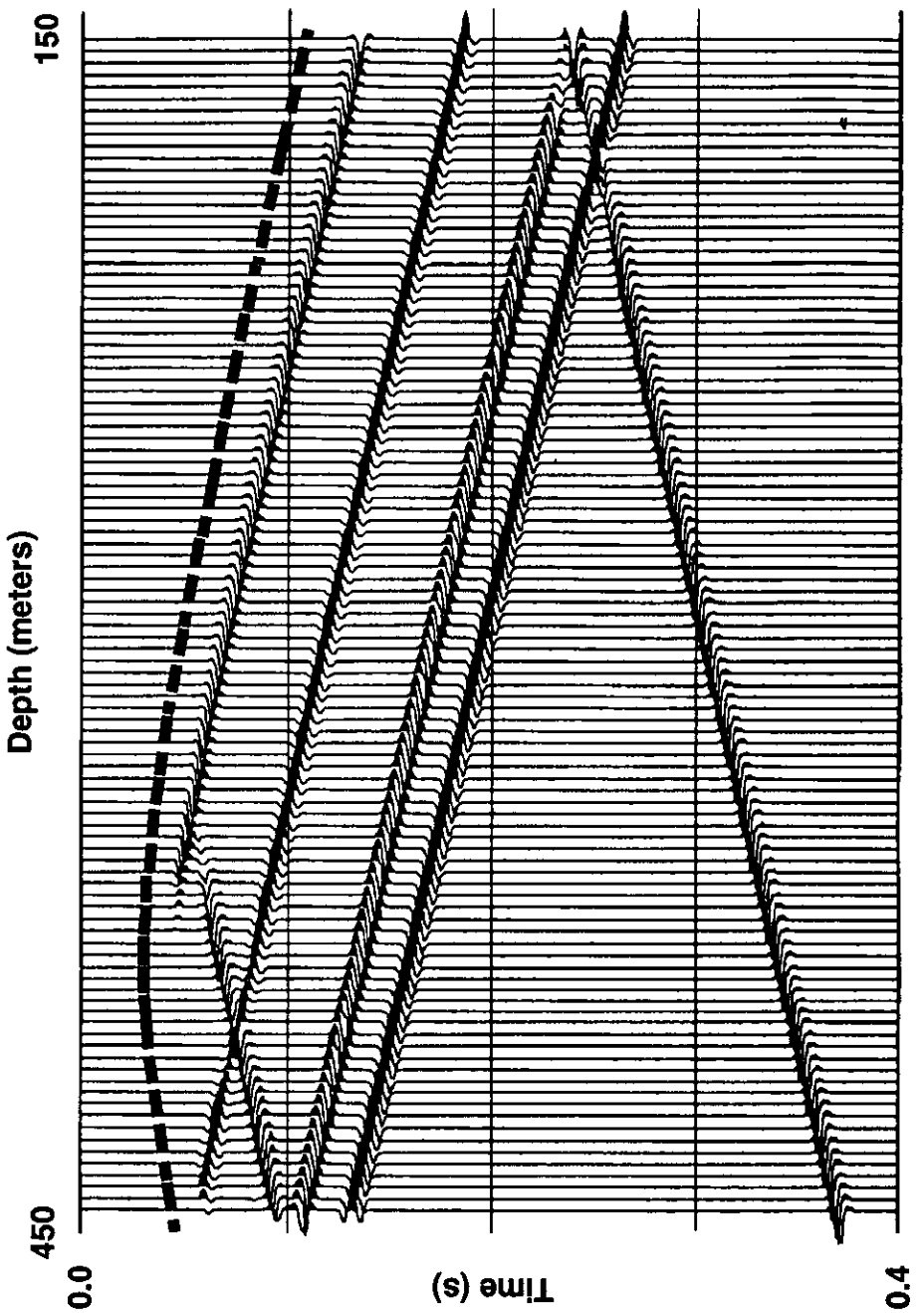

FIG. 8. Common source gather of reflection data, with the direct event (the dash line) removed by median filtering in common interval gathers.

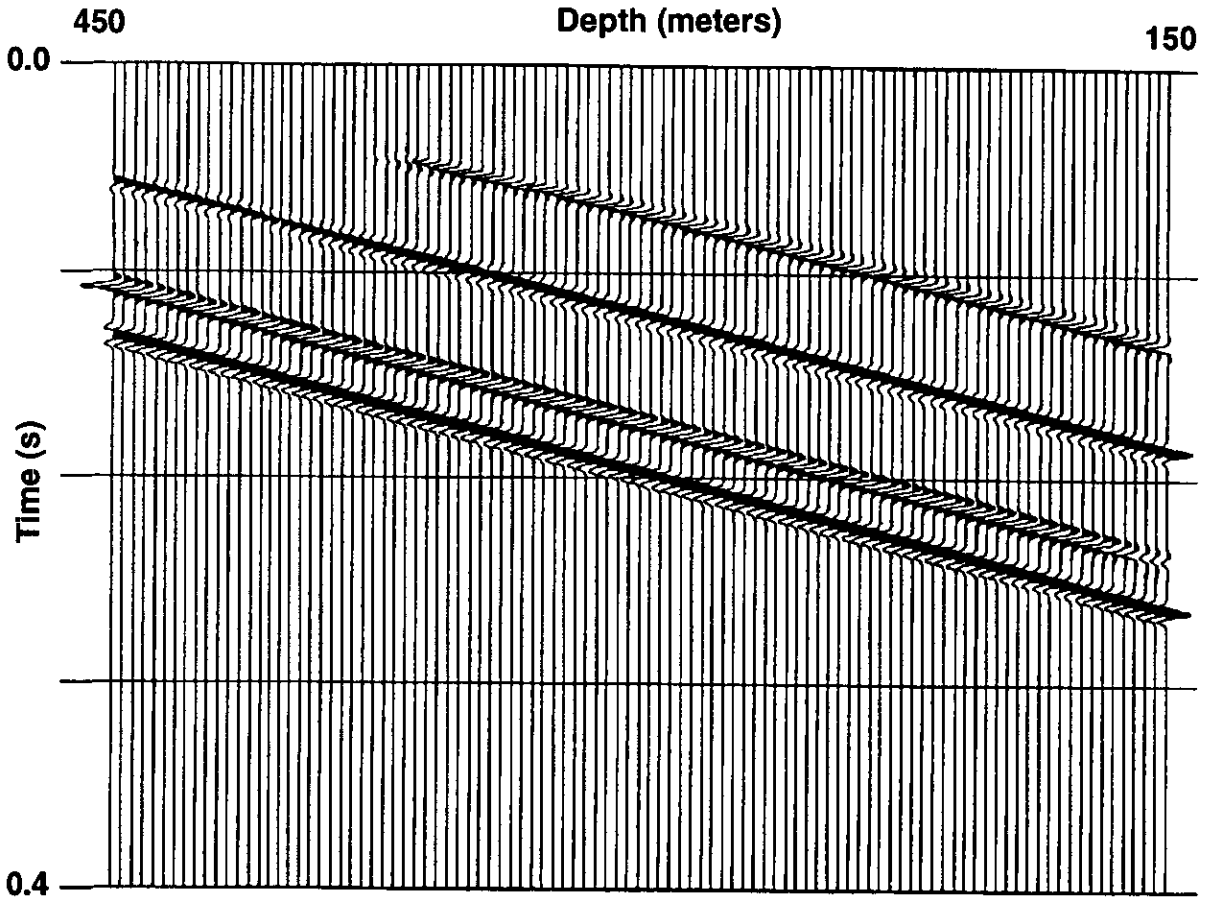

FIG. 9. Upgoing reflections in common source gather, obtained from running a f-k filter.

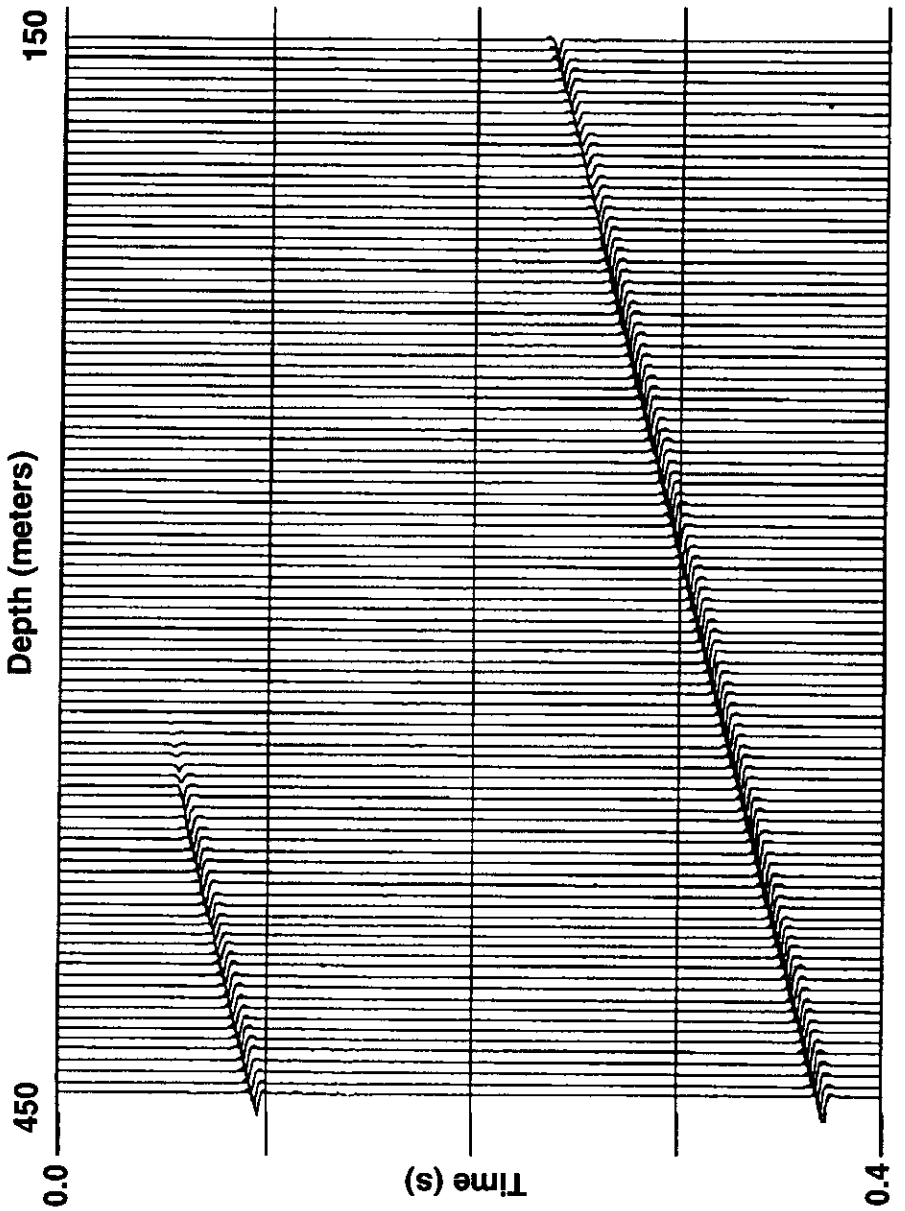

FIG. 10. Downgoing reflections in common source gather, obtained from running a f-k filter.

employed here. In the crosswell case, we used the zero-interval CI gather. A zero-interval CI gather is a collection of traces whose vertical distance between source and receiver is constant and equal to zero. Shown in Figure 11 is the synthetic zero-interval CI gather. For the sake of illustration, both upgoing and downgoing reflections are displayed in this figure, although in velocity analysis, only one type of the waves is sufficient to use for deriving velocity information from the gather. In this study, the upgoing reflection was actually used.

In the zero-interval CI case, the vertical moveout is caused by the vertical difference between adjacent traces. By scanning a set of possible velocities, the best velocity is selected that gives the best VMO correction. It means that this best velocity should cause the reflection event being considered to be best flattened.

The zero-interval gather in Figure 11 was scanned with a number of different velocities and the results are displayed in Figure 12(a) through (h). The event being considered is horizon L3 (to which the arrow points). It is seen from these displays that different velocities have different effects on VMO correction. A reflection event in a zero-interval CI gather is the reflections from the same reflection point in the subsurface. Therefore, if a correct velocity is used, this event should be flattened after the moveout correction. Let us now examine the L3 event. Looking over the eight velocities displayed in Figure 12 (a) to (h), it is found that only the velocity of 2250 m/s produces the best VMO correction for the L3 event, which now becomes flat. The 2250 m/s velocity is the one which was used in the geologic model. That means, in a constant-velocity medium, the medium velocity is the optimal moveout correction velocity. When the scanned velocity is below 2250 m/s, the event is under-corrected. On the other hand, however, if a velocity higher than 2250 m/s is used, the L3 reflection event will be over-corrected.

Note that the moveout correction velocity is dependent upon the reflector depth. It is seen from Figure 12(e) that although 2250 m/s is the best velocity for the L3 horizon, it causes under-correction for the shallower event and over-correction for the deeper reflection events. Also, note that reflections on the deeper traces (on the right side of each velocity diagram in Figure 12) are more affected by the scanning velocities than the shallower traces (on the left side), until the velocity being used is approaching closer to the best velocity. This can be conformed, for example, by comparing the L3 event in all diagrams.

CRP sorting

Reflection data, after wavefield separation, are sorted into CRP gathers according to their common lateral reflection points, determined by equation (1). Figure 13 displays two of the CRP gathers of the synthetic upgoing reflection data. When CRP gathering, a bin size of 0.5 m was used, and the reflector depth for the horizon L3 was used in equation (1). The horizontal axis of the gathers is the mid-depth for each trace, and the vertical is two-way traveltime. The bin numbers for the two gathers are respectively 49 and 51, representing a lateral CRP bin distance of 24 m and 25m, measured from the source borehole. Both gathers contain five reflection events, with the event from the top of the image zone being marked with L3. From the figure, we see that, as predicted, each reflection event shows a hyperbolic shape and that deeper events have larger moveouts than shallower events. The moveouts include the vertical and horizontal moveouts.

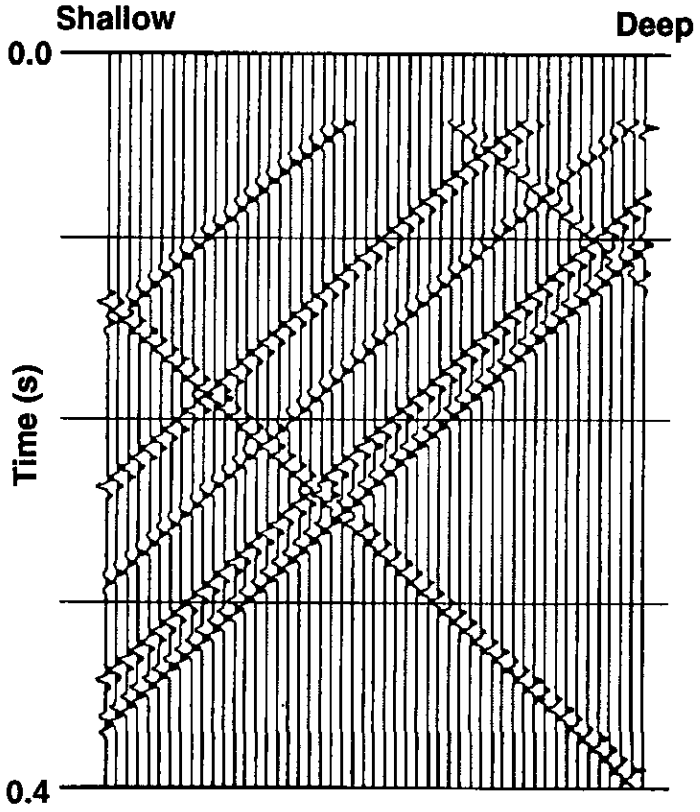

FIG. 11. A zero-interval CI gather with both up- and down-going reflections displayed.

Shown in Figure 14 is a CRP gather of downgoing reflection data, whose bin number is 49. The bin size used when gathering the data is also 0.5 m, so the bin number of 49 is equal to the horizontal distance of 24 m from the source well. The depth of the first reflector L1, i.e., the free surface of the geologic model in Figure 2, was used. In this case, it is zero. The downgoing reflection gather includes only two reflection events, one from L1, and another from L2, with the former marked. Notice the relative position of the L1 event to the L2, even though in the depth model the horizon L2 is deeper than L1. Both reflection events will be correctly re-positioned after the vertical and horizontal moveout corrections are applied, which will be discussed next. Note also the partial coverage of the event L2. The hyperbolic pattern of the downgoing reflection events, like those of upgoing reflections, are predicted theoretically.

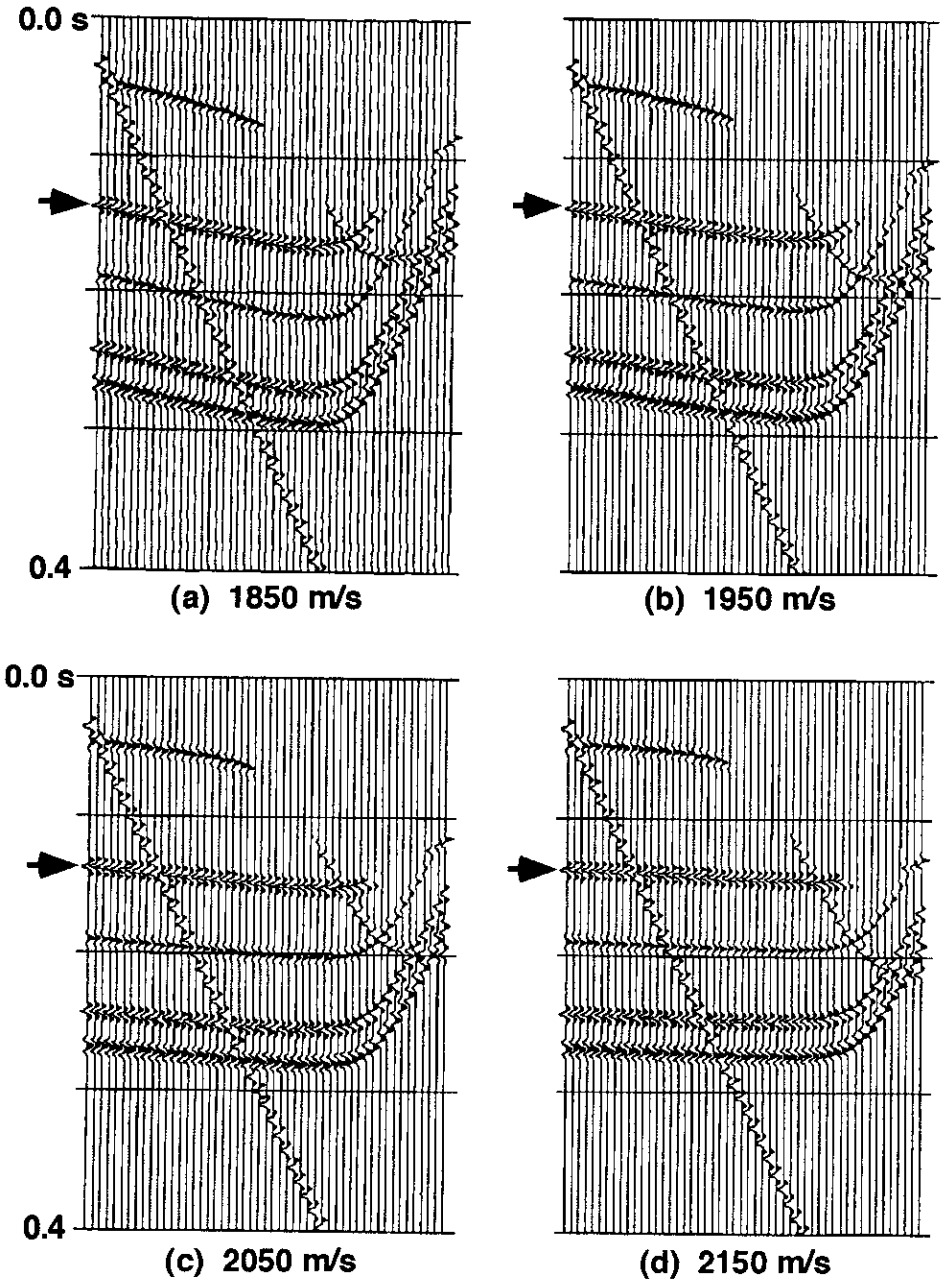

FIG. 12. Constant velocity scan in a zero-offset CI gather, in order to find the best velocity for moveout corrections. Displayed in this page are the four velocities that were scanned (a) to (d), and the other four shown in next page. Selecting the velocity of 2250 m/s, which is also the medium velocity being used, would result in the best moveout correction for the event of interest that is indicated by the arrow.

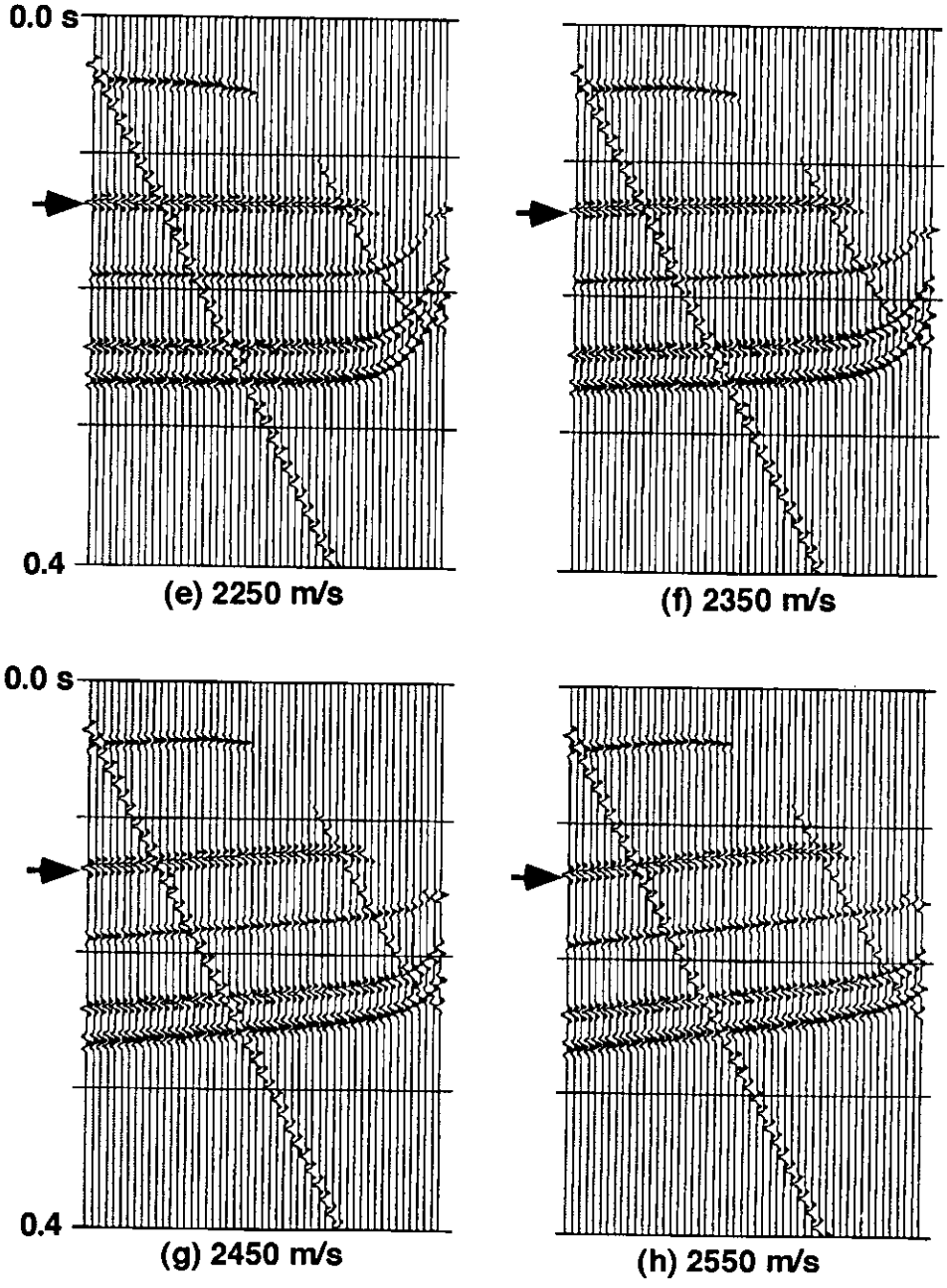

FIG. 12. Continued.

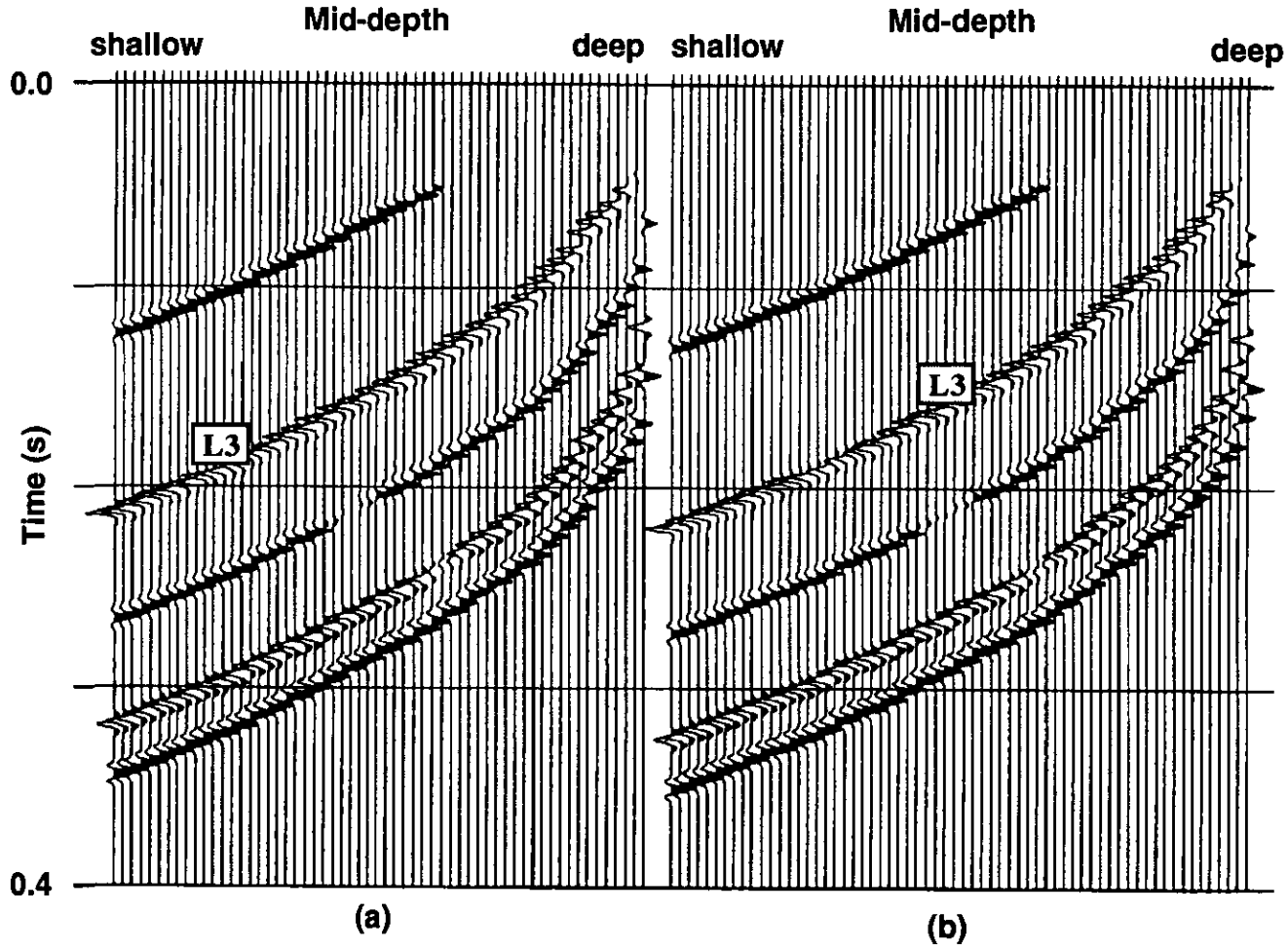

FIG. 13. Common reflection point gathers of synthetic crosswell upgoing reflection data. The CRP bin width is 0.5 m. For these two gathers, the bin number is 49 (a) and 51 (b), respectively, representing a horizontal distance of 24 m and 25 m, measured from the source well. The horizon marked L3 is top of the image zone.

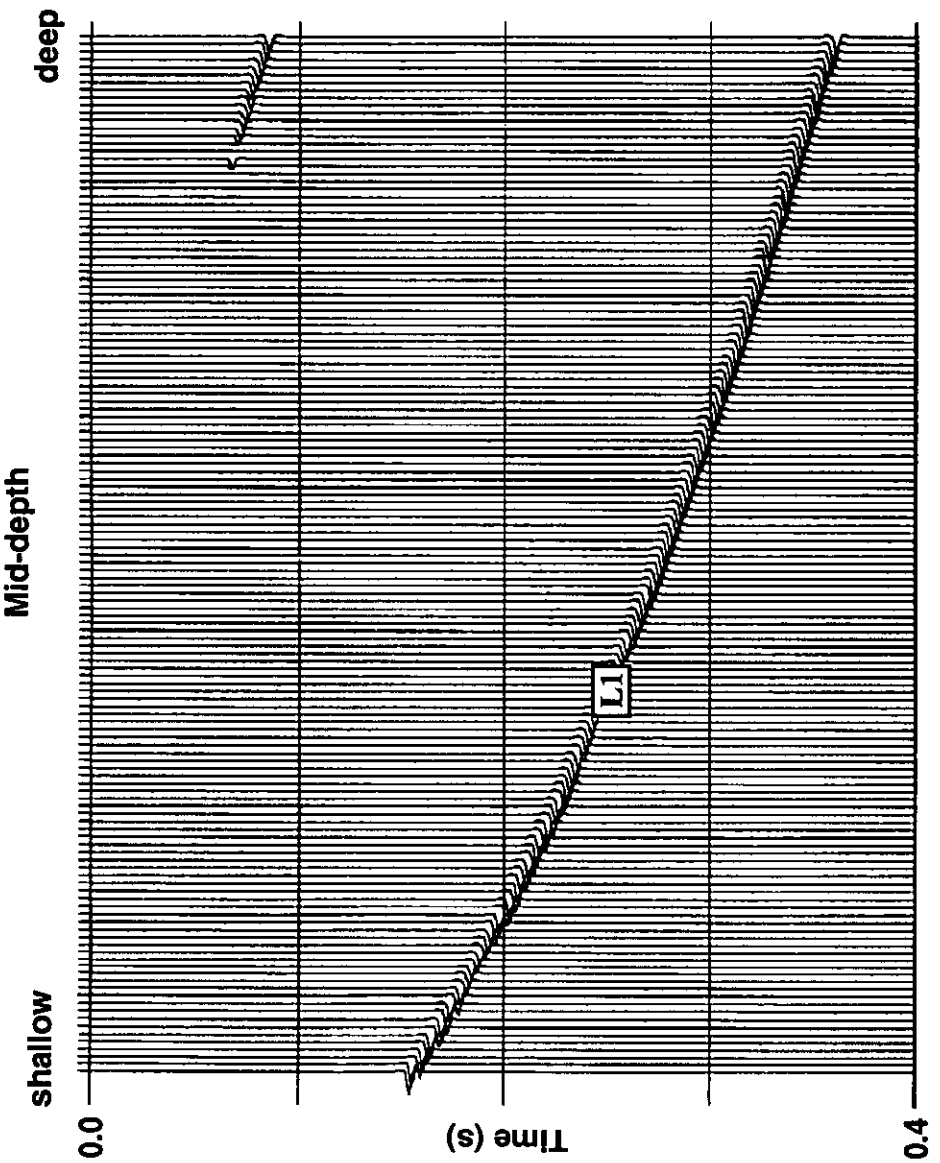

FIG. 14. Common reflection point gather of synthetic crosswell downgoing reflection data. The CRP bin width is 0.5 m. For this gather, the bin number is 49, representing a horizontal distance of 24 m, measured from the source well. The horizon marked L1 is the top surface of the geologic model.

Recall that equation (1), which determines the CRP positions, is dependent upon the depth of a reflector, D. This depth dependence determines, in turn, the dependence of CRP gathering on the reflector depths. Therefore, in each CRP gather, only one of the reflection events is actually from the same reflection point. In the case of Figures 13 and 14, the CRP gathering is true only for the event L3 (upgoing) or for the event L1 (downgoing). The rest of the events in both figures are indeed *not* from the same reflection points. This problem is a limitation of the method being discussed.

Moveout corrections

HMO correction removes the effect of the horizontal distance between the source and receiver boreholes. The amount for HMO correction is determined by equation (4). For borehole offset X, a constant of 55 m was used. The velocity for HMO correction was derived previously, and it is 2250 m/s. Figures 15 and 16 show respectively the results of applying HMO corrections to upgoing and downgoing reflection data in the CRP gathers in Figures 13 and 14. By comparing Figures 15 and 16 with Figures 13 and 14, it is found that the difference is small. This is true because in the case being considered, the borehole offset of 55 m causes just a minor horizontal moveout in the data.

Figures 17 and 18 show the same CRP gathers after vertical moveout has been corrected. The VMO velocity of 2250 m/s and the mid-depth for each trace were used in equation (5). After VMO correction, all reflection events are flattened, as expected by the theory. Applying both HMO and VMO corrections to the upgoing reflection data is equivalent to moving the source and receiver positions to a coincident location on the surface where the reflected signals, traveling vertically as shown by the dashed line in Figure 1(a), would have been recorded. This process is analogous to the NMO-corrected CDP gather case. A similar explanation can be made for the downgoing reflection situation. In the downgoing reflection gather, note that the relative position between horizons L1 and L2 has now been corrected. By VMO correction, the deeper reflection L1 now becomes a flat reflection event appearing at the time of zero, corresponding to the free surface.

More important, note that unlike the HMO and VMO processes previously discussed by Li and Stewart (1992a, b), which are dependent on the reflector depth, the HMO and VMO corrections described in this paper are independent of the reflector depth. Looking back at equations (4) and (5), it can been seen that what is required in these two moveout corrections includes only the input trace (time t), its mid-depth m, borehole offset X, and the velocity V. The dependence on the reflector depth appears only in the CRP location equation (1). Therefore, it makes this imaging method simpler and more reliable.

Imaging by stacking

Once all the traces in CRP gathers have been corrected for moveout, a horizontal stack over traces can be performed. Since upgoing and downgoing reflection data are processed separately, there should be two stacked sections. Finally, these two sections are combined for the final stacked section.

Shown in Figure 19 is a time section of upgoing reflection data. Since both VMO and HMO corrections have been applied, the data are in two-way *vertical* traveltime. The horizontal axis of the section is the bin number, representing the horizontal distance of each reflection point to the source well. In the upgoing reflection

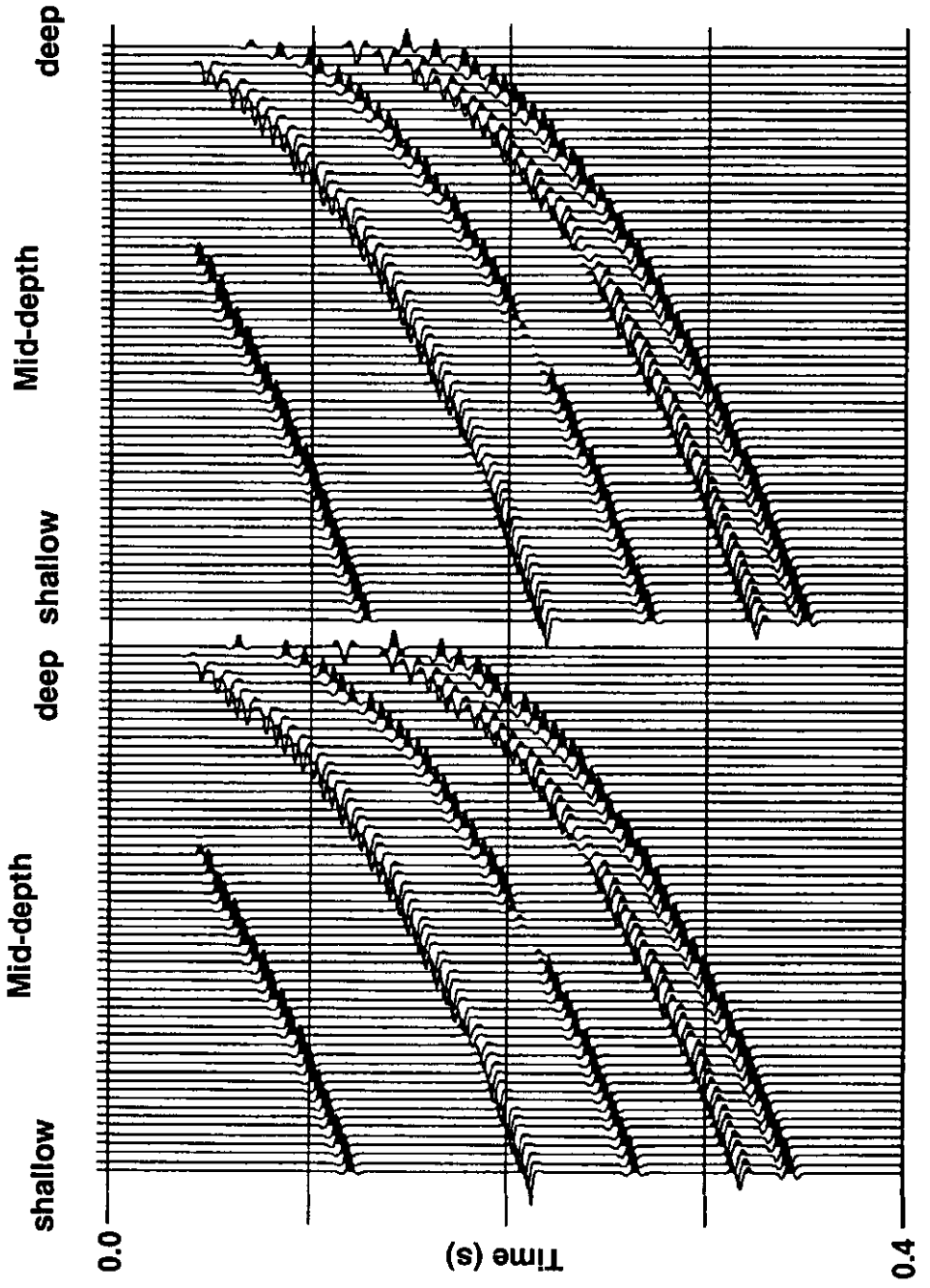

FIG. 15. Common reflection point gathers of upgoing reflection data after horizontal moveout correction.

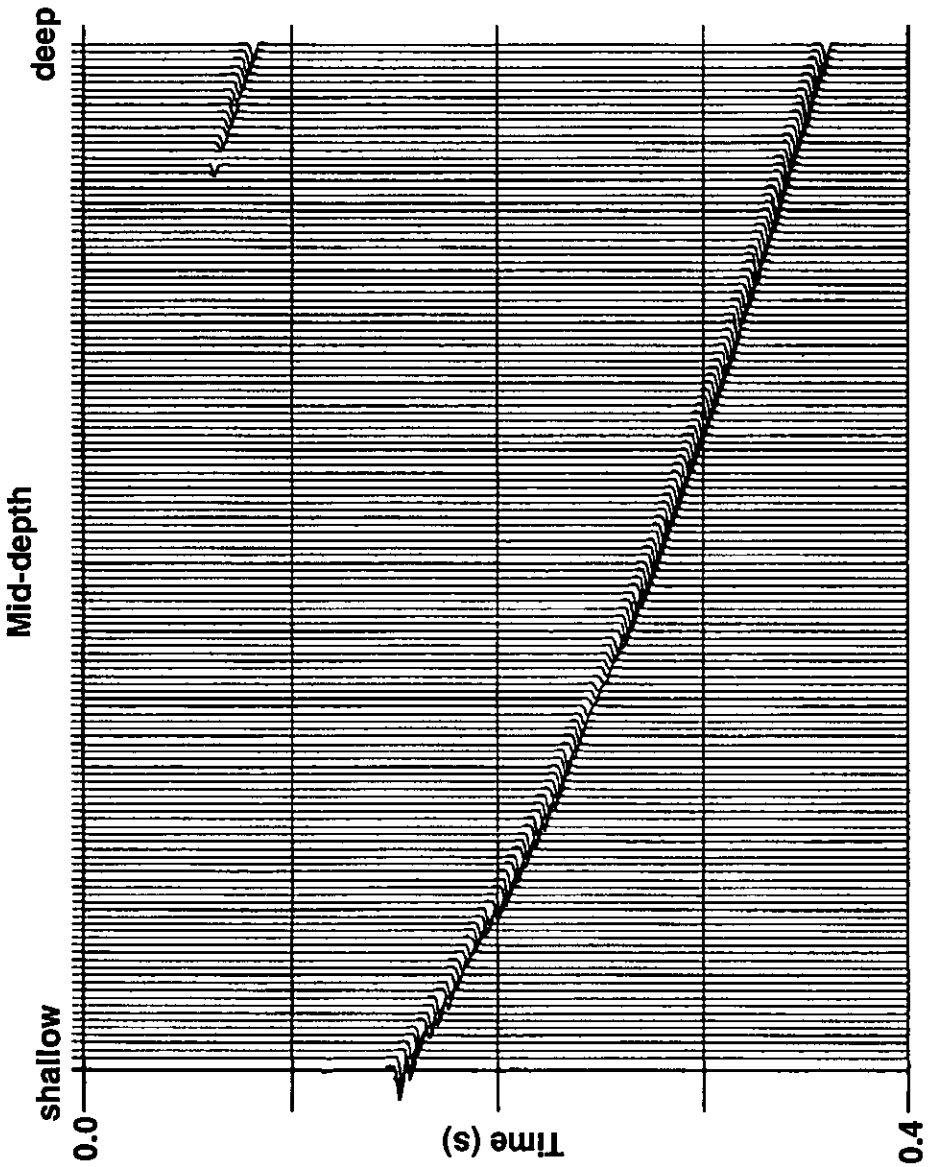

FIG. 16. Common reflection point gather of downgoing reflection data after horizontal moveout correction.

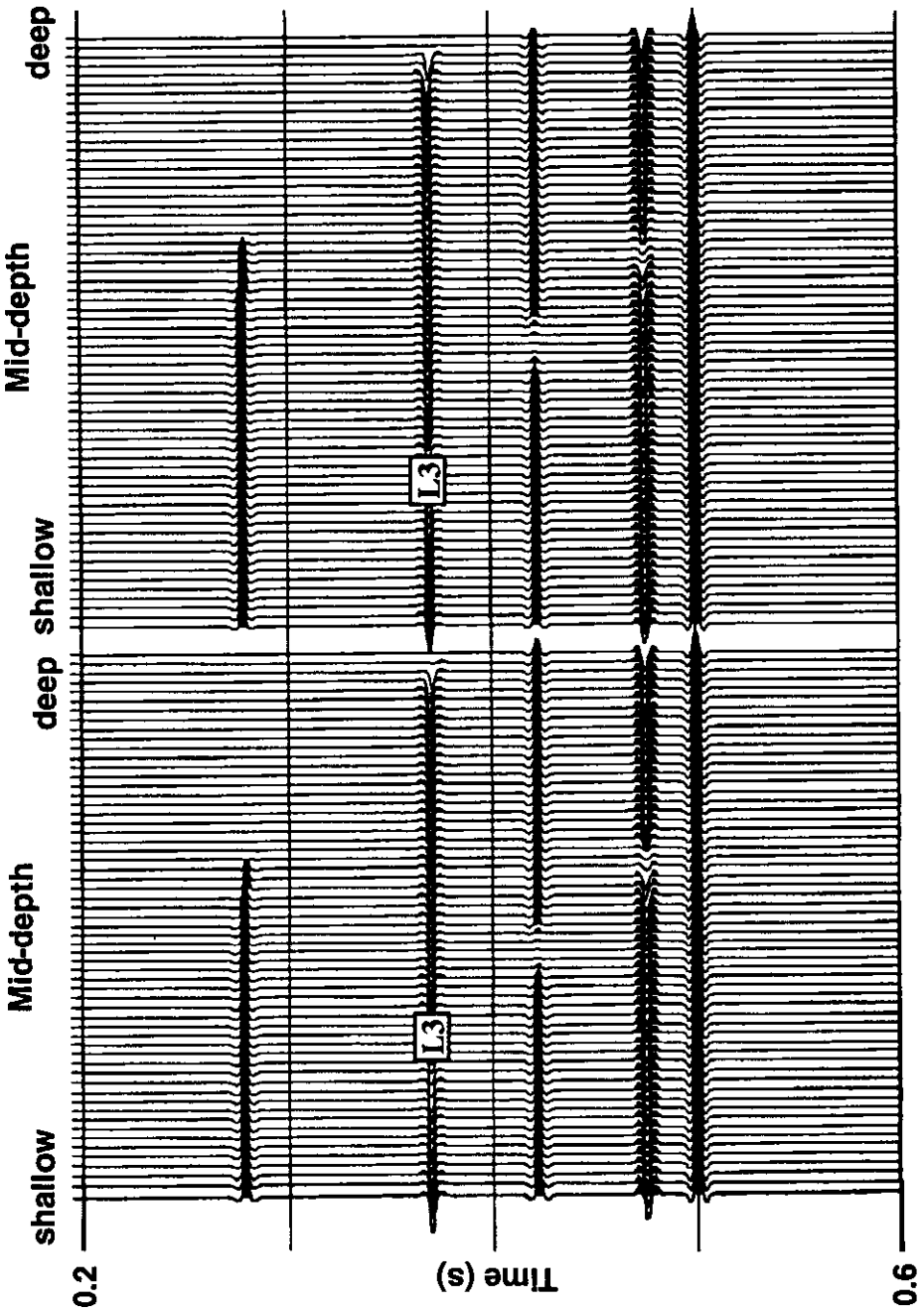

FIG. 17. Common reflection point gathers of upgoing reflection data after vertical moveout correction, which flattens the reflection events.

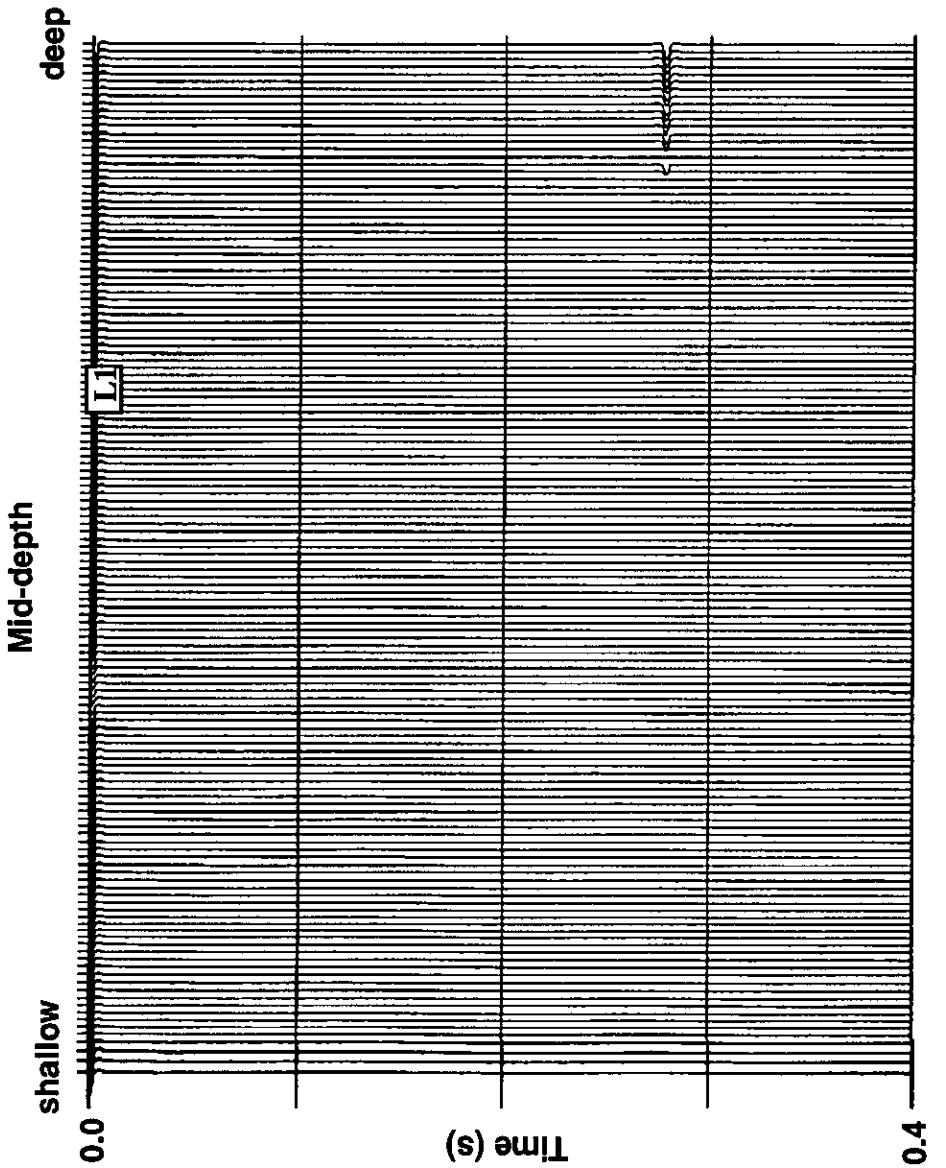

FIG. 18. Common reflection point gather of downgoing reflection data after vertical moveout correction, which flattens the reflection events and moves them into their correct positions.

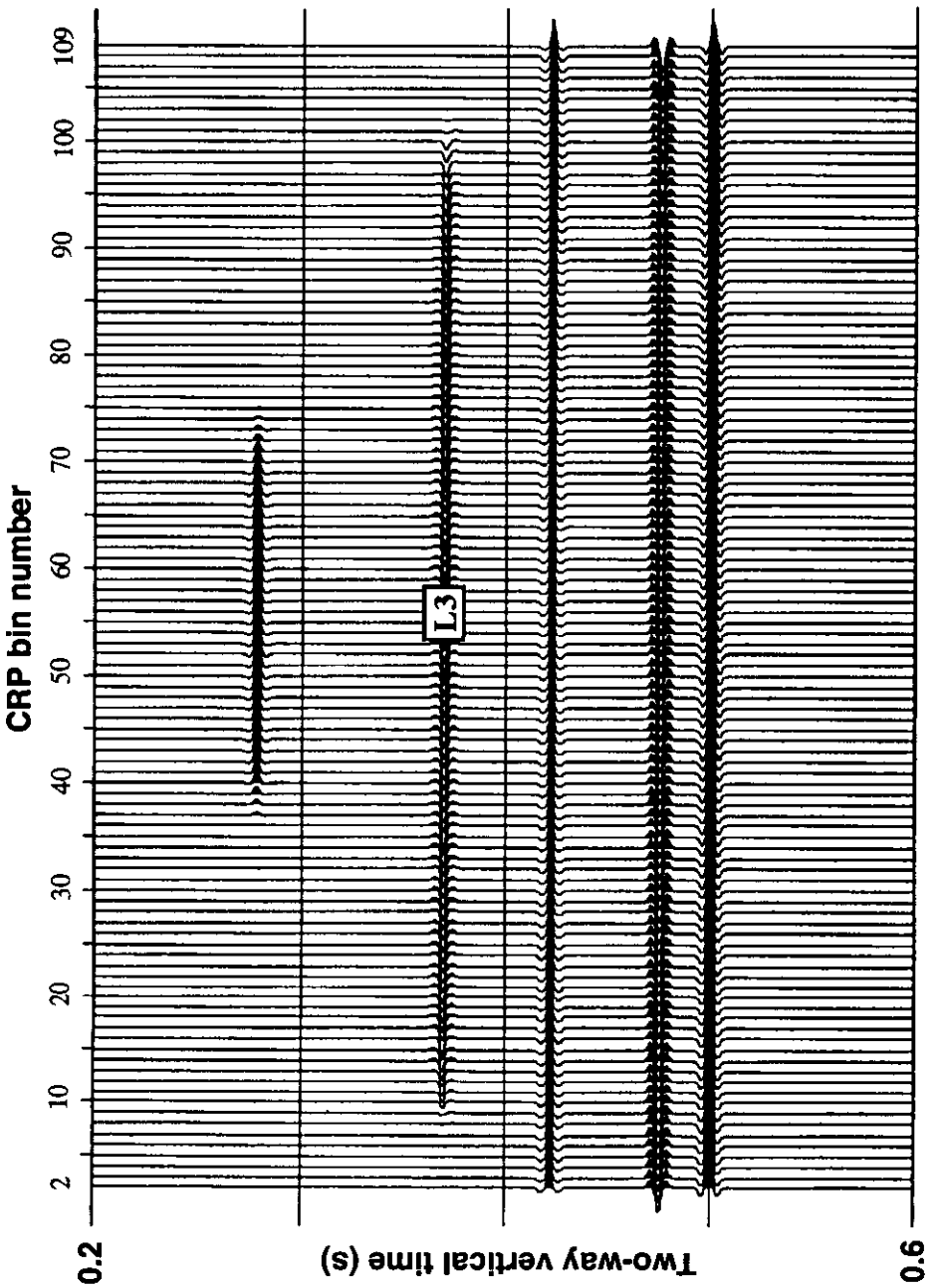

FIG. 19. Time stack section of upgoing reflection data.

case, the bin number starts from 2, and ends at 109, indicating a range of 53.5 m between two borehole that has been imaged. In the section, five reflection events are seen, representing reflectors L2 to L6, from shallow to deep. Except the shallowest event (L2), the rest are well imaged. Note the coverage of the top and bottom (L3 and L4) of the image zone. The stacked section for downgoing waves is given in Figure 20, where reflections from the free surface (L1) and the reflector L2 are imaged, with a negative polarity. It is necessary to reverse the polarity of the downgoing reflection data when constructing a final time section which combines the up- and down-going reflection data. The final time stacked section is displayed in Figure 21.

A depth section is also produced after a time-depth conversion is carried out. The depth section will give an actual representation of the depth model. The depth section is given in Figure 22. An AGC of 600 ms was applied. Displayed together with the section is the geologic model for comparison. From either time or depth section, it can be seen that a very good image of the depth model has been reconstructed through the crosswell reflection data processing. Although the shallow reflectors are partially imaged, due to the limitation of the coverage in the crosswell geometry, deep reflectors are well imaged. Therefore, crosswell reflection imaging potentially provides a powerful means in imaging subsurface geology.

To overcome the depth-dependent problem as encountered before, a composite stacked section could be generated. The composite stacked section is generated in such a manner that CRP gathers are formed from a number of different reflector depths, moveout corrections are applied to them, these gathers are stacked to yield a number of stacked sections focusing on different reflectors and finally, these sections are combined to give a single composite stacked section. Figure 22 is actually a composite depth stacked section. The depths for horizons, L2 and L3, were used. A stacked section was generated for each depth and then combined altogether. Note the wider coverage of these horizons in the composite section, compared to the horizons in the time section in Figure 21, which focused only on L3.

The processing flow is summarized in Figure 23.

CONCLUSIONS

In this paper, we have outlined a processing flow for crosswell seismic data. The procedure has used data in several kinds of gathers, such as common interval gathers, common source gathers, and common reflection point gathers. The CRP stacking method is introduced and easy to implement. This method involves a few processing steps, including: 1) Sorting separated reflection data into CRP gathers; 2) Correcting for horizontal moveout; 3) Correcting for vertical moveout; and 4) Stacking. The processing flow is tested on synthetic crosswell seismic data. This synthetic study has shown that this processing procedure is very effective in imaging subsurface reflectors. It is expected that this procedure should work reasonably well for real crosswell seismic data.

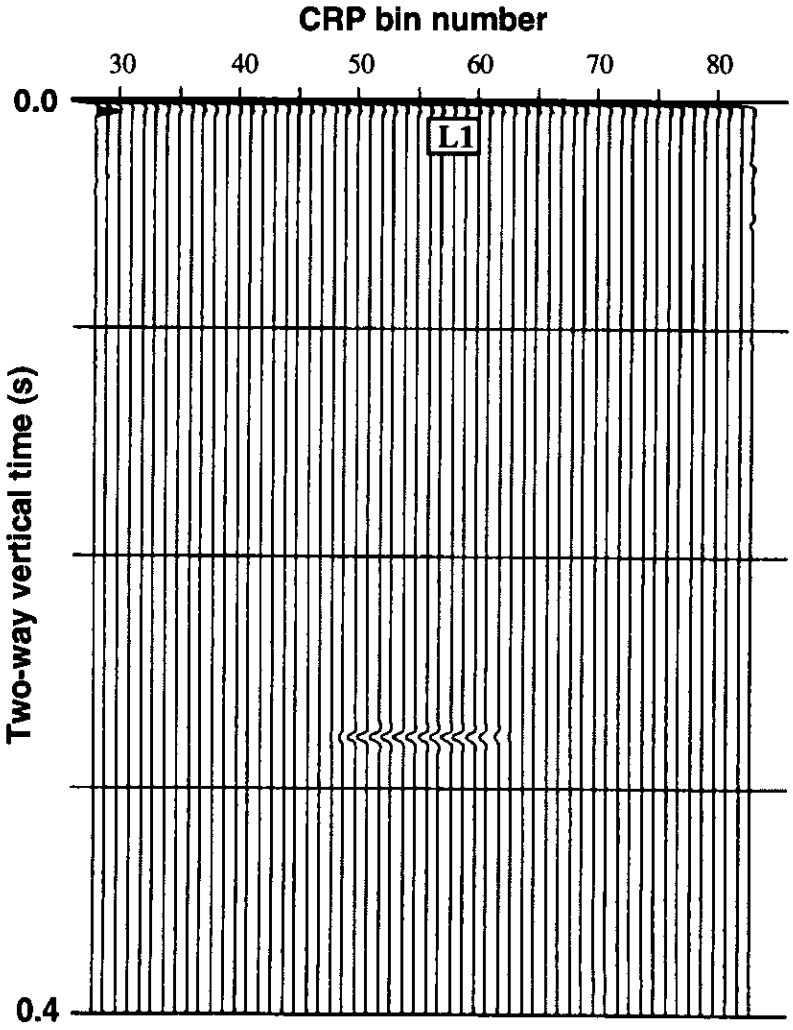

FIG. 20. Time stack section of downgoing reflection data.

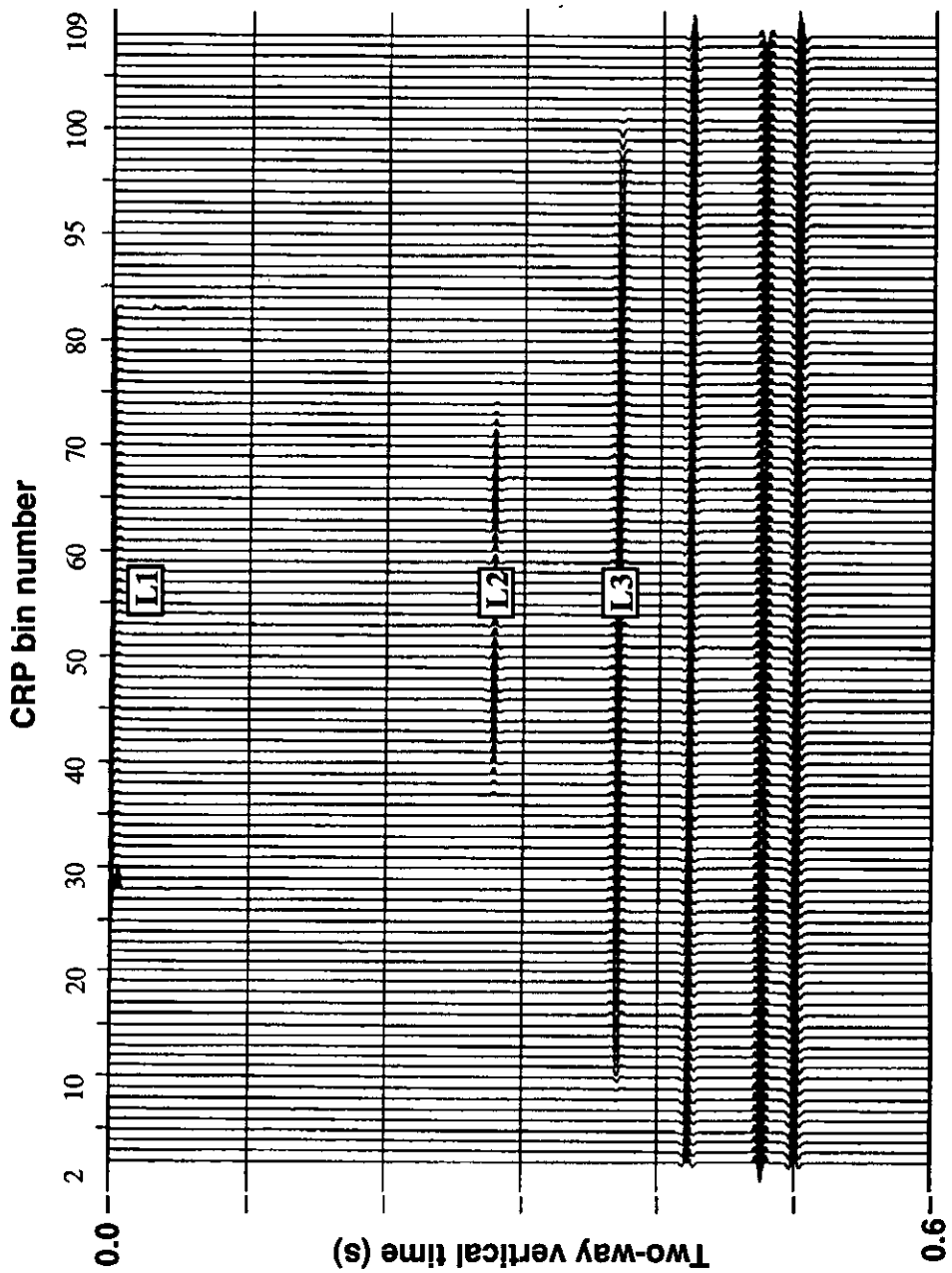

FIG. 21. Time stack section containing upgoing and downgoing reflection data.

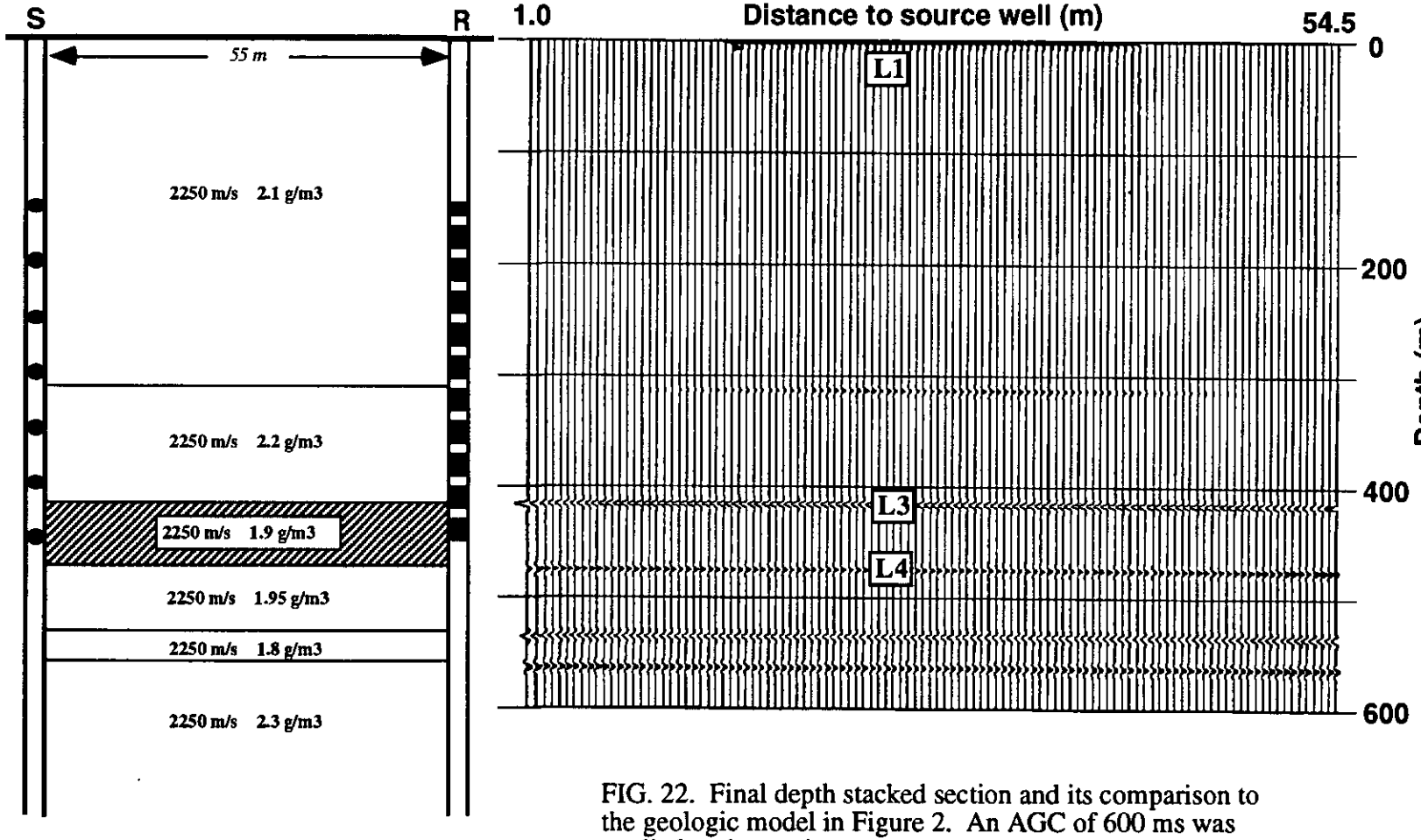

FIG. 22. Final depth stacked section and its comparison to the geologic model in Figure 2. An AGC of 600 ms was applied to the section.

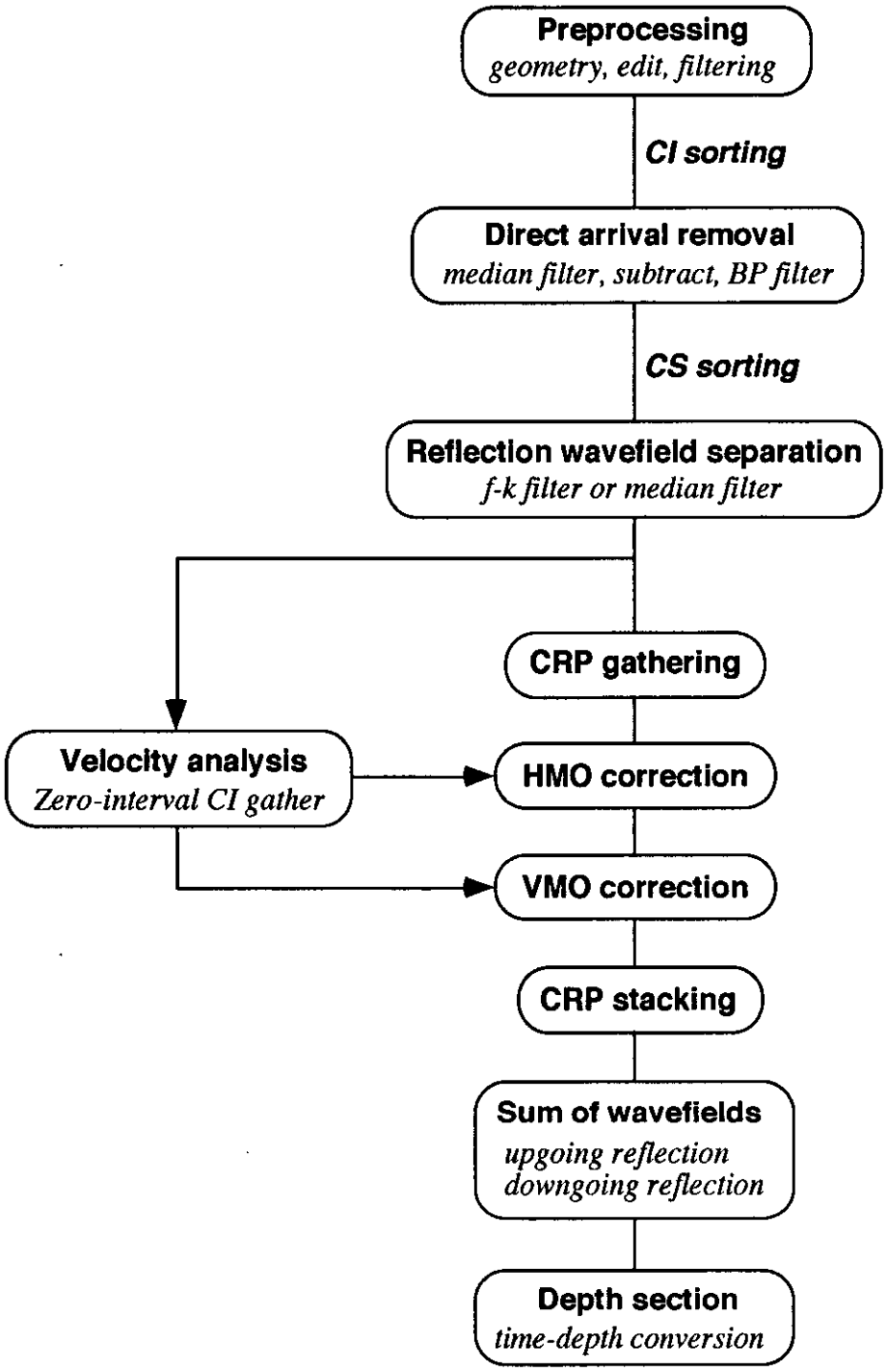

FIG. 23. Processing flow chart for the common reflection point stacking method.

REFERENCES

Abdalla, A. A., Stewart, R. R., and Henley, D. C., 1990, Traveltime inversion and reflection processing of cross-hole seismic data: presented at the 60th Ann. Internat. Mtg., Soc. Expl. Geophys.

Bregman, N. D., Bailey, R. C., and Chapman, C. H., 1989, Crosshole seismic tomography: Geophysics, **54**, 200-215.

Hu, L., McMechan, G. A. , and Harris, J. M., 1988, Acoustic prestack migration of cross-hole data: Geophysics, **53**, 1015-1023.

Iverson, W. P., 1988, Crosswell logging for acoustic impedance: Journal of Petroleum Technology, January, 75-82.

Khalil, A. A., Stewart, R. R., and Henley, D. C., 1993, Full-waveform processing and interpretation of kilohertz cross-well seismic data: Geophysics, **58**, 1248-1256.

Lazaratos, S. K., Rector, J. W., Harris, J. M., and Van Schaack, M., 1991, High-resolution imaging with cross-well reflection data: Presented at the 61st SEG Intern. Ann. Mtg., Houston.

Lazaratos, S. K., Rector, J. W., Harris, J. M., and Van Schaack, M., 1992, High resolution crosswell imaging of a west Texas carbonate reservoir: part 4: reflection imaging: Presented at the 62nd SEG Intern. Ann. Mtg., New Orleans.

Li, G., and Stewart, R. R., 1992 a, Imaging the subsurface using crosswell seismic reflection data: A synthetic study: Presented at the 1992 CSEG Convention, Calgary, Alberta.

Li, G., and Stewart, R. R., 1992 b, Crosswell reflection imaging: CREWES Project Research Report, Vol. 4, The University of Calgary.

Li, G., and Stewart, R. R., 1993, Reflection imaging for crosswell seismic data: Friendswood, Texas: CREWES Project Research Report, Vol. 5 , The University of Calgary.

Lines, L. R., and LaFehr, E. D., 1989, Tomographic modeling of a cross-borehole data set: Geophysics, **54**, 1249-1257.

Lines, L. R., and Tan, H., 1990, Cross-borehole analysis of velocity and density: presented at the 60th Ann. Internat. Mtg., Soc. Expl. Geophys.

Peterson, J. E., Paulsson, B. N. P., and McEvilly, T. V., 1985, Applications of algebraic reconstruction techniques to crosshole seismic data: Geophysics, **50**, 1566-1580.

Pratt, R. G., and Goulty, N. R., 1991, Combining wave-equation imaging with traveltime tomography to form high-resolution images from crosshole data: Geophysics, **56**, 208-224.

Qin F., and Schuster, G. T., 1993, Constrained Kirchhoff migration of cross-well seismic data: Presented at the 63th SEG Ann. Intern. Mtg., Expanded Abstracts, Washington, D. C.

Stewart, R. R., 1985, Median filtering: review and a new F/K analogue design: J. Can. Soc. Expl. Geophys., **21**, 54-63.

Stewart., R. R., Marchisio, G., and Li, G., 1991, Crosswell seismic imaging: Fundamentals and a physical modeling study: Presented at the 1991 CSEG Convention, Calgary, Alberta

Stewart, R.R., and Marchisio, G., 1991, Cross-well seismic imaging using reflections: Presented at the 61st SEG Intern. Ann. Mtg., Houston.

Zhou, C., and Qin F., 1993, Real data crosshole reverse-time migration: Presented at the 63th SEG Ann. Intern. Mtg., Expanded Abstracts, Washington, D. C.